UNIVERSITÀ DEGLI STUDI DI PARMA

DIPARTIMENTO DI FARMACIA

DOTTORATO DI RICERCA IN
BIOFARMACEUTICA-FARMACOCINETICA

DRUG COMBINATION: PHARMACEUTICAL TECHNOLOGIES APPLIED TO THE MANUFACTURING OF COMBINED DOSAGE FORMS FOR ORAL ADMINISTRATION

Coordinator: Chiar.mo Prof. Ruggero Bettini

Tutor: Chiar.ma Prof.ssa Alessandra Rossi

Co-tutor: Chiar.mo Prof. Paolo Colombo

PhD Candidate: Giulia Pasotti

XXVIII CICLO

1. Introduction

1.1. Urinary system

The urinary apparatus is the system that includes all organs involved in the formation, storage and voidance of urine. The main functions of this system are to remove waste products from the body (mainly urea and uric acid), regulate the electrolyte balance (e.g. sodium, potassium and calcium), regulate the acid-base homeostasis, control the blood volume and maintain blood pressure. The urinary system is composed by kidneys, which function is the production of urine, by collecting ducts, ureter, bladder and urethra which function is storage and subsequently expel urine from the body by urination (Figure 1).

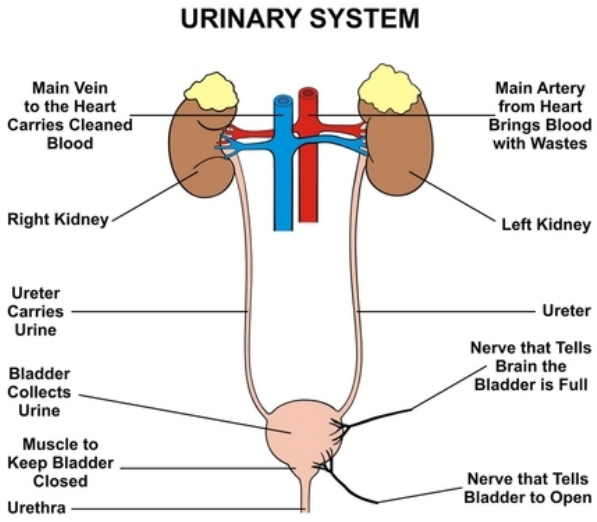

Figure 1: Urinary system: structure and functions [1].

The female and male urinary systems are very similar, differing only in the length of the urethra [2]. In female subjects, the urethra is about 4 centimeters

long and ending at the vulva, the area of the external female genital organs. It constitutes exclusively a route of urine excretion. In male subjects, the urethra runs the length of the penis, is about 20 centimeters long and opens at the end of the penis (glans). The male urethra is used to eliminate urine as well as semen during ejaculation [3].

1.2. Benign prostatic hyperplasia

One of the most common diseases of old-aged men regarding this system is the Benign Prostatic Hyperplasia (BPH), also known as Benign Prostatic Enlargement. It is a non-cancerous increase of prostate size (Figure 2). BPH involves hyperplasia of prostatic stromal and epithelial cells, resulting in the formation of large, fairly discrete nodules in the transition zone of the prostate [4].

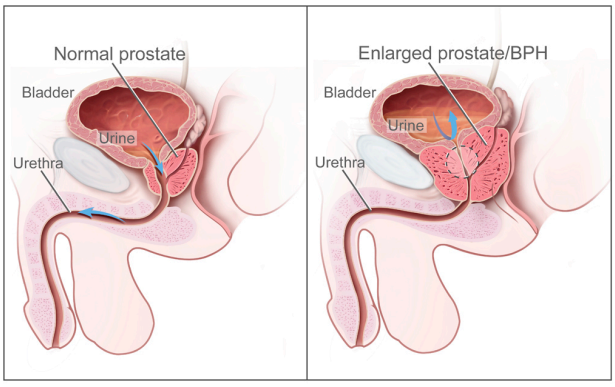

Figure 2: Normal and enlarged prostate [5].

The clinical manifestations of an enlarged prostate include lower urinary tract symptoms (LUTS), bladder outlet obstruction, incomplete bladder emptying, acute and chronic urinary retention, urinary tract infection (UTI), urosepsis,

bladder stones, and hematuria [6].

The prevalence of BPH histopathology is aged-dependent, with initial development usually after 40 years of age (no cases were observed in patients under the age of 30), as demonstrated in a study conducted in 1984 by Berry and colleagues [7]. Approximately more than 50% of men aged 60 and up to 90% of those between 70 and 80 years show some symptoms of BPH [8].

A review of the literature provides compelling evidence that the prevalence of histologic BPH is similar throughout the world [9]. BPH is one of the most common diseases of aging men, ranking in the top 10 most commonly diagnosed conditions in men over 50 years [10]. BPH, through its associated LUTS, can be very distressing and bothersome to those affected [11]. Men with severe symptoms of BPH have poor health status and their quality of life might be afflicted in varying degrees [12]. Although this condition is rarely life threatening, it has an enormous economical impact. Approximately one in five men with BPH will have a significant clinical event, such as acute urinary retention of prostate surgery, within one year of initiating treatment for BPH [8]. The average employee with a diagnosis of BPH misses 7.3 hours of work annually related to his disease, with 10% reporting some work loss related to healthcare encounters for the pathology [13]. It has been estimated that the annual costs of caring for BPH exceed $4 billion in the United States [14].

A proper and timely diagnosis of this disease may slow down its progression and help to monitor its development.

Currently, different methods are available for the diagnosis of BPH [15]:

- Urine test

- Level in the blood of prostate-specific antigen (PSA), produced only by the prostate gland
- Post-void residual volume (PVR) of the urine left in the bladder after urinating
- Measurement of the urine flow by uroflowmetry
- Cystoscopy of the urethra and bladder
- Urodynamic pressure in the bladder during urinating

Patients with mild symptoms may not require treatment. Moderate symptoms can be treated with a variety of medications that relax the smooth muscle of the prostate. Men with more advanced symptoms may require additional treatments as a surgical procedure. Undiagnosed and untreated, the condition can lead to chronic inflammation of the prostate and even to kidney failure. Occasionally, BPH is associated with unwelcome side effects, such as incontinence and impotence.

Pharmacological management is the most common therapeutic approach for patients with benign prostatic hyperplasia. Alpha-blockers and 5-alpha-reductase inhibitors are the most prescribed in the initial treatments [16]. Alpha-blockers as doxazosin, terazosin, alfuzosin, tamsulosin and silodosin, are the most common choice [17]. All these drugs are equally effective but have slightly different side effect profiles [18]. Alpha-blockers act relaxing smooth muscle in the prostate and the bladder neck, thus decreasing the blockage of urine flow. They affect the action of endogen catecholamines on prostate stromal smooth muscle, where α_{1A} receptors are present, reducing the smooth muscle tone and extent of obstruction [19]. All the α-blockers, available on the market for several

years, have been extensively studied; although head-to-head comparative studies are rare, they are currently regarded as equally clinically effective drugs in improving patient symptoms, patient quality of life due to LUTS, and maximum flow rate, as demonstrated by systematic review performed by the Cochrane Collaboration and AUA guidelines panel [20]. The most common side effects of these molecules include orthostatic hypotension, headaches, ejaculation changes, nasal congestion, and weakness. Non-selective alpha-blockers such as terazosin and doxazosin may also require titration (gradually adjusting the dose of a medication) as they can cause fainting if the dose is too high. Side effects can also include erectile dysfunction [21].

Finasteride and dutasteride, belonging to the 5-alpha-reductase inhibitors family, are another treatment option [22, 23]. These molecules inhibit 5-α-reductase, which in turn inhibits production of dihydrotestosterone, a hormone responsible for enlarging the prostate. Effects may take longer to appear respect to α-blockers. When the 5-alpha-reductase inhibitors are used together with the alpha-blockers, benefits were reported not in short-term trials, but in longer term studies (3-4 years): there was a greater reduction in BPH progression to acute urinary retention and surgery than with agents alone, especially in patients with more severe symptoms and larger prostates [24, 25]. Side effects include decreased libido and ejaculatory or erectile dysfunction [26].

Antimuscarinics such as tolterodine may also be used, especially in combination with alpha-blockers [27]. They act by decreasing acetylcholine effects on the smooth muscle of the bladder, thus helping to control symptoms

of an overactive bladder [28].

Phosphodiesterase (PDE) inhibitors (i.e. tadalafil and sildenafil) have shown promise as useful drugs. In a study the inhibition by tadalafil of 5-PDE, which is mainly expressed in the stromal compartment of the prostate, reduced proliferation of primary prostate stromal cells and led to a lesser extent of primary prostate basal epithelial cells [29].

Several studies have demonstrated the efficacy of sildenafil citrate in treating lower urinary tract symptoms concomitant erectile dysfunction that are often correlated with BPH [30].

1.3. Silodosin

The active ingredient silodosin (Figure 3) is commonly used for the symptomatic treatment of bening prostatic hyperplasia.

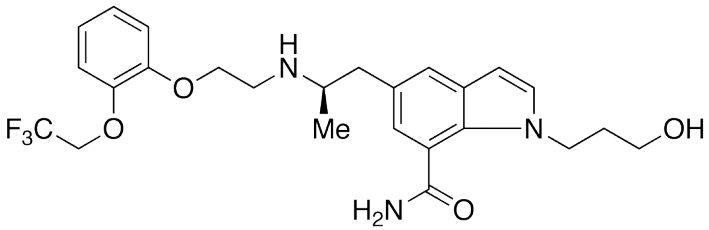

Figure 3. Chemical structure of silodosin.

Silodosin is an alpha-blocker, that acts as an α_1-adrenoceptor antagonist with high uroselectivity, in particular for the prostate [31].

The α_1-adrenoceptors (α_1-AR) were identified in many human tissues and they are copious in the smooth muscle of the prostate. Until today there has been discovered only three kinds of α_1-AR (α_{1A}, α_{1B} and α_{1D}), but there are data that show the existence of a fourth category of these receptors (α_{1L}), which role has

still to be established [32]. An in vitro study, using Chinese hamster ovary cells, showed the binding affinity of silodosin with cloned human α_1-adrenergic receptor subtypes and with the prostatic tissue [33].

Silodosin works by relaxing smooth muscles in the prostate and bladder, with the consequent reduction of the resistance of the bladder outlet, without compromising the contractility of the detrusor smooth muscle. It follows an improvement in symptoms of lower urinary tract associated with the filling (irritation) and emptying (obstruction) of the bladder, which helps to improve urine flow and reduce symptoms of BPH [34].

Alfuzosin, doxazosin and terazosin are usually considered non-selective drugs, inhibiting all the different α_1-receptor subtypes. Conversely, tamsulosin and, above all, silodosin have higher selectivity for α_{1A} receptors [20].

Major differences do exist in the adverse events of these different drugs. Compared to other drugs of the class of inhibitors of α-adrenergic receptors (including alfuzosin, terazosin and tamsulosin), normally used for the treatment of BPH, silodosin shows a lower reduction of blood pressure (0.2 mmHg), practically comparable to patients treated with placebo. In addition, after treatment with silodosin, an improvement in urine flow and quality of life is observed. In clinical trials the most common adverse effects were reported more frequently in the group of patients treated with silodosin than with placebo are retrograde ejaculation, dizziness, weakness, sore throat, diarrhea, incontinence and headache [35].

Silodosin was discovered by Kissei Pharmaceutical Co. Ltd and it received the first marketing approval in Japan in 2006 under the trade name of Urief®. In

October 2008 the FDA approved its use in the USA for the treatment of LUTS in association with BPH and was marketed under the name of Rapaflo®. In January 2011 the European Commission approved silodosin for the symptomatic treatment of BPH (Silodyx®, Urorec®).

Silodosin is administered orally in immediate-release capsules, once a day, preferably in the morning after meal, to minimize the risk of side effects such as orthostatic hypotension. The recommended dose in Europe and the USA is 8 mg/day, except for patients with moderate renal failure, for which the initial dose is 4 mg/day. In Japan, the dose is 2 or 4 mg twice a day. Silodosin is quickly absorbed and has a bioavailability of approximately 32% when administered at 8 mg/day. The administration of the drug with food decreases the value of C_{max} by about 30% and increases t_{max} of about 1 hour; this is the reason why it is recommended to take silodosin with food [36]. After administration of 8 mg once a day for 7 days the following pharmacokinetics parameters were measured:

- C_{max} 87 ± 51 ng/mL
- t_{max} 2.5 h
- AUC 433 ± 286 ng h/mL
- V_d 0.81 L/kg

Silodosin is bound for about 97% to plasma proteins. It shows a significant first-pass effect, 55% is excreted in the faeces and 34% by the kidney, mostly as metabolites and only about 5% as unmodified silodosin. Its half-life and its main metabolite (silodosin glucuronide) are about 11 and 18 hours, respectively. However, plasma levels of silodosin decrease rapidly during the first 2-3 hours and then decreases more slowly (biphasic trend). In Figure 4 the plasma

concentration profiles after oral administration of capsules, containing different doses of silodosin, are shown [37].

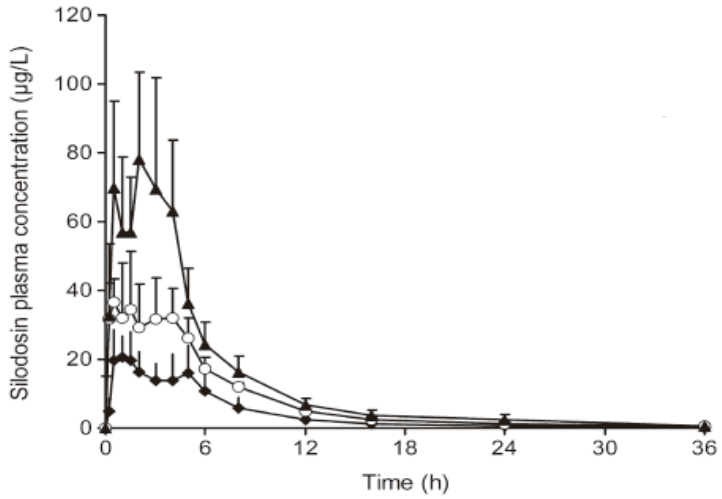

Figure 4. Profiles of plasma concentration vs. time after oral administration of capsules containing single dose of silodosin of 4 mg (◆), 8 mg (○) and 12 mg (▲); n=10) (modified from [37]).

However, the two most common side effects, such as dizziness and retrograde ejaculation due to the loss of the "compression chamber" derived from pharmacological relaxation of the bladder neck, are more frequent as a result of use of silodosin than tamsulosin. Given that the problems associated with erectile dysfunction might be present in patients with symptoms of lower urinary tract, it might be recommended the association of silodosin with phosphodiesterase-5 inhibitors as sildenafil.

1.4. Sildenafil Citrate

Sildenafil citrate (Figure 5), trade name Viagra®, is a molecule developed by the pharmaceutical company Pfizer. It is commonly used for the treatment of

erectile dysfunction and, most recently, of pulmonary arterial hypertension (Revatio®) [38].

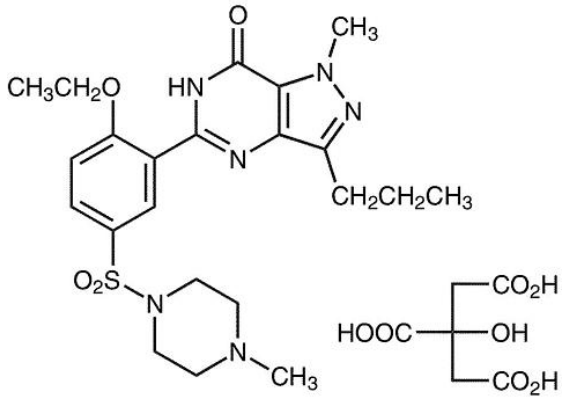

Figure 5. Chemical structure of sildenafil citrate.

At the beginning it has been studied to treat hypertension and *angina pectoris,* but during the clinical trials showed low efficacy for the treatment of *angina* but high effects on the erectile function of penis.

The molecule was patented in 1996 and approved for use in erectile dysfunction by the FDA in 1998. The mechanism action of sildenafil citrate is to protect cyclic guanosine monophosphate (cGMP) from degradation by cGMP-specific phosphodiesterase type 5 (PDE-5) in the corpus cavernosum located in the penis. Nitric oxide (NO) in the corpus cavernosum binds to guanylate cyclase receptors, which results in increased levels of cGMP, leading to smooth muscle relaxation (vasodilation) of the intimal cushions of the helicine arteries. This smooth muscle relaxation leads to vasodilation and increased inflow of blood into the spongy tissue of the penis, causing an erection [39].

Clinical studies have established a physiological relation between LUTS and the symptoms related to BPH. In patients suffering from LUTS in association with

BPH it was observed that sildenafil citrate, phosphodiesterase-5 inhibitors, has an additive action with silodosin [40-42]. The two actives have a complementary mechanisms of action: the α_1-lithic stops the formation of inositol phosphate and decreases the levels of intracellular Ca^{2+} by relaxing the smooth muscle of the prostate; the phosphodiesterase-5 inhibitor increases the concentration of cyclic GMP (guanosine-cyclic monophosphate) and the release of nitric oxide which can relax the smooth muscles of the prostate. As a consequence of these results, the combination of a phosphodiesterase-5 inhibitor with an antagonist of α_1-adrenergic receptor leads to a significant improvement of symptoms in patients affected by BPH and LUTS.

According to BCS classification, sildenafil citrate is a drug of class I. Sildenafil, after oral administration, is rapidly adsorbed in the intestine. The blood concentration of the drug reaches the maximum values within an hour. Its bioavailability is about 40% due to the hepatic first pass effect. After oral administration of 50 mg of the drug the following pharmacokinetic parameters were measured [43]:

- C_{max} 159 ng/mL
- t_{max} 1.46 h
- AUC 530 ng h/mL
- k_e 0.17 h^{-1}

Sildenafil is bound over 95% to plasma proteins and its half-life is approximately 3.5 hours. The plasma concentration profiles after intravenous and oral administration of 50 mg of sildenafil citrate are shown in Figure 6 [43].

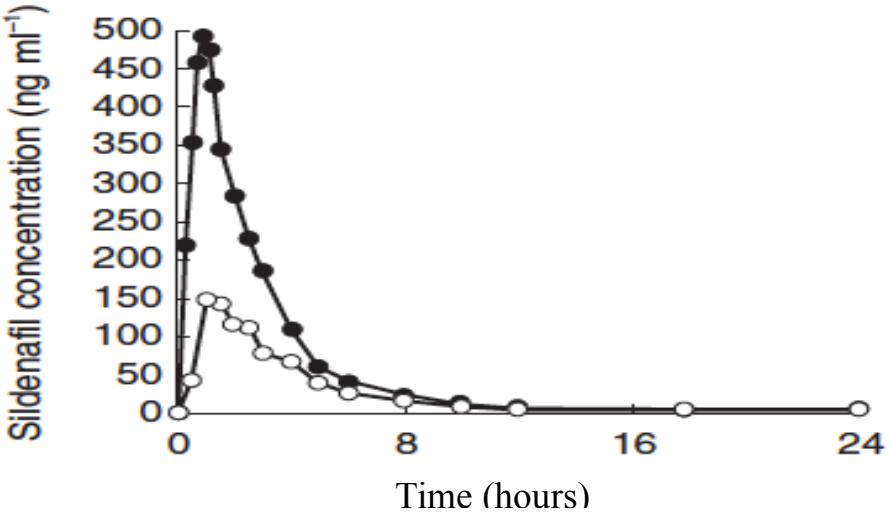

Figure 6. Profiles of plasma concentration vs. time after oral (○) and intravenous (●) administration of 50 mg of sildenafil (n=12) (modified from [36]).

Transport studies of sildenafil citrate in rabbit intestinal membrane showed a greater absorption of the drug in the small intestine compared to the colon [44]. The administration of sildenafil in gastro-retentive dosage forms could increase its bioavailability.

It was observed in a study conducted on healthy men that, the co-administration of silodosin with maximum therapeutic doses of sildenafil citrate in two different dosage forms did not evidence clinically significant pharmacodynamics interactions [45]. Co-administration did not appear to be associated with clinically important changes in orthostatic pressure. Thus, the co-administration of the two drugs might be an appropriate treatment for BPH patients who experience erectile dysfunction.

1.5. Modified Release Solid Oral Dosage Forms

Among all drug delivery systems, oral delivery is the most convenient and commonly preferred route for administration of several drugs. It has some

specific advantages characteristics, such as ease of administration (can be self-administered), pain free, flexibility in the design and low cost.

In the last few decades, pharmaceutical research has focused its attention to the necessity to modify drugs release. Modified or controlled release oral drug delivery systems have been shown to offer advantages over conventional system [46]. Some problems correlated with the conventional drug delivery system are:

- Poor patient compliance, increased chances of missing the dose of a drug with short half-life for which frequent administration is necessary (especially for chronic disease);
- Fluctuations of drug concentration levels that may lead to under or over medication;
- Difficult on the attainment of steady-state condition;

Controlled release can overcome various issues tied to the conventional release, changing the kinetics of drug release, offering prolonged delivery of drugs and maintenance of plasma levels within the therapeutic range. Oral modified release dosage forms are developed by altering the drug release to achieve predetermined clinical objectives. Possible therapeutic benefits of a modified release product include improved efficacy, reduced side effects, increased patient compliance, optimized performance and reduced dosing frequency. Several formulations capable to control both the rate and the site of drug release have been studied.

Oral modified release dosage forms can be divided in three different categories:

1. *Delayed release*: the drug is released after a certain interval of time after administration;
2. *Extended release*: the drug is released slowly over time;
3. *Pulsatile release*: the drug is released in sequential way and repeated in the time.

In this way it's possible to obtain constant drug release rate reducing drug level fluctuations in blood and maintain a steady state concentration over a prolonged period of time.

Furthermore, drug plasma levels are kept within a narrow window with no sharp peaks, with a subsequent reduction of adverse side effects, of the dose frequency and an improvement of patient compliance. Thus, it is possible to target the drug delivery to its site of absorption or action, reducing unwanted side effects [47].

1.6. Hydrophilic matrix systems

Among the various modified-release pharmaceutical forms designed for the oral route, the most widespread is the one constituted by swellable matrix systems. The active ingredient is dissolved or dispersed in a swellable hydrophilic polymer able to swell and dissolve in contact with an aqueous solvent [48-53]. These systems are commonly manufactured by direct compression, wet or dry granulation and hot melt extrusion. The choice of the type of polymer to be used determines the control of release. The polymer acts as a control element of the issue, and must meet certain requirements such as biocompatibility, mechanical

strength and permeability to the drug [54]. The polymers more frequently used are some cellulose esters (hypromellose, hydroxypropyl cellulose and sodium carboxymethylcellulose), polyethylene oxide, carbomers, sodium alginate and xantham gum [55]. Drug release from these delivery systems is basically regulated by solvent-polymer interaction and solvent-drug interaction. The polymer primarily used for the production of swellable matrix is hydroxypropylmethylcellulose (HPMC, Figure 9) due to its technological characteristics, availability, handling and use, reduced toxicity and cost [56].

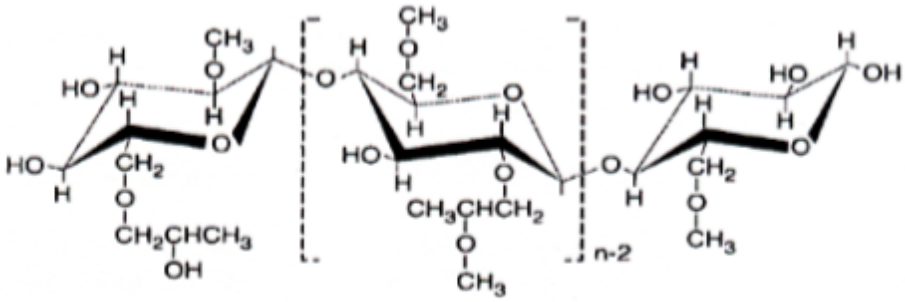

Figure 9. Structure of hydroxypropylmethylcellulose.

The HPMC is a hydrophilic polymer capable of absorbing large quantities of water. The characteristics of the polymer, in particular the degree of viscosity, the amount, the size of the particles and the solubility, affect the release of the drug from the matrix [57]. The different viscosity of HPMC depends on the degree of substitution by methyl and hydroxypropyl groups that affect the interaction of the chains of the polymer with water, and then the hydration of the matrix. If the polymer has a high viscosity it has more rapid hydration and forms quickly a layer of dense and thin gel at the beginning, which decreases the entry of water and then the release of the drug [58,59]. When the content of

HPMC in the matrix reaches high percentages (30-40%), the degree of substitution becomes less influential on the release kinetics of the drug. High polymer content causes the formation of a gel layer that slowly erodes by controlling the release of the drug; a small amount of polymer allows a greater penetration of water into the matrix and a consequent increase in rate of drug release.

Also the polymer particles size, affects the speed of hydration of the polymer itself modifying the release of the drug. Small polymer particles lead to the formation of dense matrix because of the bonds between the particles while large particles lead to a high porosity and therefore to a fast release of the drug due to a slow hydration of the particles and to the formation of a uneven gel which causes the disintegration of the matrix. The swelling of the matrix occurs when the system is placed in contact with an aqueous solvent, such as a biological fluid, and is influenced by the penetration of solvent into the polymer that allows the transition from the glassy state to the rubbery state as a result of the relaxation of the polymer chains [60-62]. The transition from glassy to rubbery state is accompanied, as well as by swelling, also by the formation of a layer of gel on the outer surface of the matrix which hinders simultaneously the water uptake and the release of drug.

The swelling of these matrices can be described by the position of the fronts, inside the matrix, due to the changes of the physical state of the polymer and/or the drug (Figure 10) [63].

Usually, starting from the centre of the matrix, three fronts can be observed:

• *Swelling front*: boundary between the dry core and the swollen matrix;

• *Diffusion front*: boundary between the undissolved solid drug and the drug in solution within the gel layer. It is more common to observe the diffusion front if the drug has limited water solubility;

• *Erosion front*: boundary between the matrix and the dissolution medium [63].

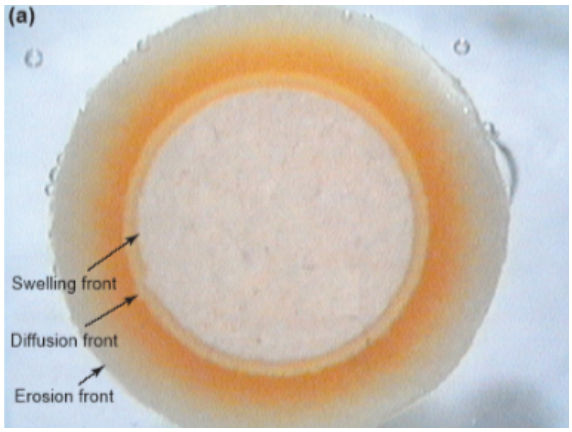

Figure 10. Image of a HPMC containing 60% (w/w) buflomedil pyridoxal phosphate taken after 4 hours of swelling [64].

The relative movement of erosion and swelling fronts determines the thickness of the gel layer and drug release rate and kinetics, since drug release occurs by diffusion through the gel layer. The fronts are continuously in motion and this is associated to physical phenomena that follow one another within the matrix:

- he movement of the swelling front depends on the speed with which the water enters into the matrix;
- the diffusion front changes position based on the rate of drug dissolution;
- the erosion front moves following the dissolution of the polymer, when the polymer chains are distant from each other and surrounded by the solvent.

At the beginning, the erosion front moves outward to the solvent, while the swelling front moves inwards as a result of water penetration. Thus, at the early stage of the dissolution process, the gel thickness increases. As the hydration

process continues, the erosion front moves inwards, in the same direction of the swelling front, because of the progressive dissolution of polymer chains in the medium. If the rate of movement of both fronts is the same, the gel thickness is constant. In this phase, the synchronization of the two fronts produces a constant drug release. Finally, when the entire polymer is swollen, only erosion occurs and the gel thickness decreases until the matrix is completely dissolved [65]. The presence of a visible diffusion front depends on the drug solubility. If the drug is highly soluble, it easily dissolves in the small volume of water present in the gel layer. Therefore, undissolved drug is present only in the dry core of the matrix and the diffusion front coincides with the swelling front. Otherwise, for poorly soluble drugs, the diffusion front is observed within the swollen gel layer. The movement of this front depends on the drug solubility: it tends to be faster when the drug solubility is higher, providing also higher release rate. In addition, drug solubility affects also the thickness of the diffusion front and its rate of change. In systems where a diffusion front is present, the polymer relaxation near the swelling front may be reduced by the undissolved drug. Here the drug dissolution and its subsequent diffusion through the gel layer is more important in controlling drug release than the gel thickness [63].

It is observable that the performance of a matrix system, in terms of drug release rate and release kinetics, is highly influenced by the nature of the drug and the polymer used in the formulation. In addition to the characteristics of the polymer and of the drug, the factors that affect the release of drug from the matrix include the solubility of the excipients, the size and shape of the matrix, the relationship between surface area and volume of the matrix.

The release of the drug from the matrix is controlled by the interaction between water, polymer and drug [66]. The polymer is mainly responsible for the release kinetics of the drug, because its characteristics affect the speed of the matrix swelling and the viscosity of the gel layer that the drug has to cross. The characteristics of the drug that influence the release are the solubility and the particle size. More the drug is soluble faster will be its release.

1.7. Release kinetics

The release kinetics of drug from a swellable and erodible matrix has been described by Ritger and Peppas [67-69] through the following mathematical model (eq 1):

$$\frac{M_t}{M_\infty} = kt^n \qquad \text{eq. 1}$$

where M_t is the drug released at time t, M_∞ is the quantity of drug released at infinite time, k is a constant related to the geometric and structural characteristic of the matrix, n is the release exponent that describes the mechanism of drug release.

The n value is used to characterize different release for cylindrical shaped matrices and it characterizes the release mechanism of drug. The value of n = 0.5 represents system where the Fickian diffusion is the main mechanism of release (Case I), 0.5 < n < 1 describes Anomalous-Fickian release where both diffusion and relaxation mechanism contribute to drug release, n = 1 indicates Zero order release (Case II) if the drug is released upon relaxation of the hydrated polymeric chains and n > 1 indicates Super Case II release. Case II

release refers to transport of drug solute via the erosion of polymeric matrix due to relaxation of polymer chains, whereas anomalous release to the summation of both drug diffusion and polymer erosion or swelling-controlled drug release. The extreme values of 0.5 and 1 are valid only for matrices with the geometry of a thin film. For cylindrical matrices *n* takes the value of 0.45 for diffusion-controlled release and 0.89 for relaxation-controlled release [70,71].

Another interesting model by Peppas and Sahlin (eq. 2), that considered the two phenomena controlling the release as additive, was proposed [72]:

$$\frac{M_t}{M_\infty} = k_1 t^m + k_2 t^{2m} \qquad \text{eq. 2}$$

where M_t / M_∞ is the fraction of drug released at time *t*, k_1 is the constant related to the diffusional contribution, k_2 is a constant related to the relaxation of the polymer chains, *m* is the diffusional exponent related to the geometry of the system.

The mathematical description of the entire process of drug release from a swellable matrix remains rather difficult, because of the number of physical characteristics that must be taken into consideration, such as water penetration into the matrix, polymer swelling and dissolution, erosion process, drug dissolution and diffusion, radial and axial transport in 3-dimensional system, moving fronts and changes in matrix dimension, porosity and compositions.

1.8. Dome matrix technology

With the advances in pharmacogenomic and pharmacogenetic sciences, individualized therapy is met with challenges of having dosage form that can be

mixed and matched to meet the intended drug regimen and pharmacokinetics requirements [73]. From the therapeutic point of view, the personalization of therapy addresses the specific health needs and personal of the individual patient.

In 2006, Colombo et al [74] developed an innovative modular technology platform where the single-unit dosage form design can be constructed through the assembly of the required drug matrix modules into a single unit for controlled drug release via the oral route.

The Dome Matrix module is constituted of a cylindrically shaped tablet or matrix, with two bases, one concave and the other convex (Figure 11). The axial section of the module appears as a dome, hence the name of Dome Matrix.

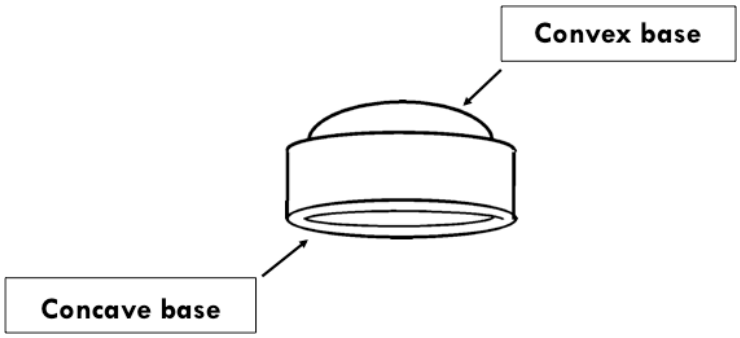

Figure 11: Dome Matrix module.

Principally, the individual modules are designed to allow the convex base of one module to be inserted in the concave base of another. There are two different types of modules, identified as male and female module, differing from each other from the concave base design.

Female Module

Two different female modules can be obtained. The first one, terminal module (Figure 12), allows only the interlocking of a male or female module into its concave base. In contrast, the second type (Figure 13) besides being able to accommodate a module into the base concave, can be stacked on its convex base thanks to the particular geometry of this face, into the concave base of another module female [74].

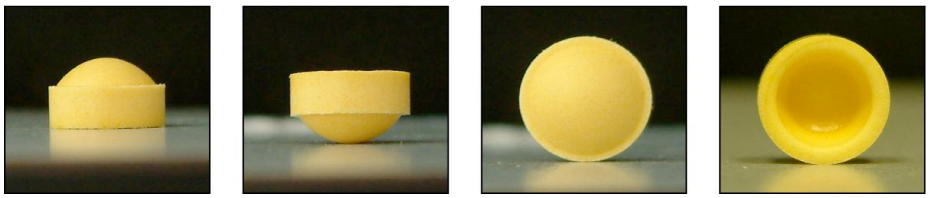

Figure 12: Dome Matrix terminal female module.

Figure 13: Dome Matrix stackable female module.

Male Module

The male modules (Figures 14 and 15) are characterized by the presence of an annular protrusion on the concave rim base, which allows the interlocking with the concave face of female modules.

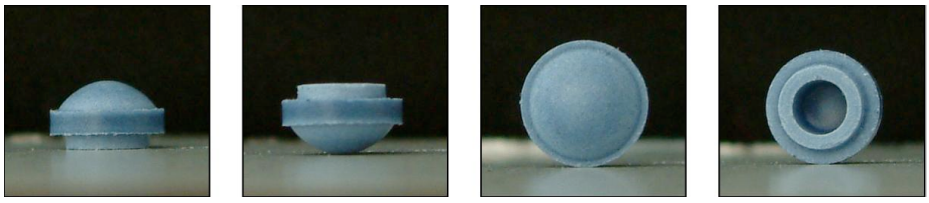

Figure 14: Dome Matrix terminal male module.

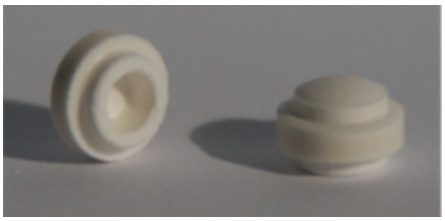

Figure 15: Dome Matrix stacked male module.

1.8.1. Dome Matrix assembling configurations

The modules assembling may take place in different ways, it depends by the features of the two modules: piled configuration, void configuration and mixed configuration.

Stacked Configuration

This type of configuration is obtained putting the convex base of a module into the concave base of another (male or female stacked with female module) (Figure 16).

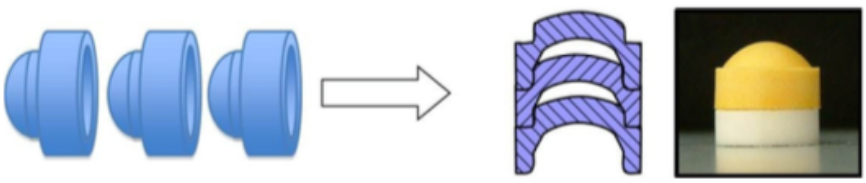

Figure 16: Dome Matrix modules assembled in stacked configuration.

In this way is possible the assemblage of more modules to control the drug release rate thank to the relationship volume/surface exposed to the dissolution medium.

Void Configuration

The Void Configuration is obtained by interlocking the annular protrusion of a male module with the concave base of a female module (Figure 17).

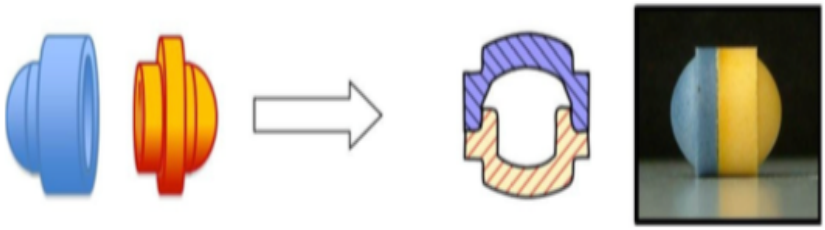

Figure 17: Dome Matrix modules assembled in void configuration.

This configuration is characterized by an inner empty space that provides buoyancy of the assembled system, obtaining delivery systems able to float on the gastric-content that perform drug release in the stomach (Figure 18) [75,76]. A configuration of this kind can be useful for the drugs with an absorption window and site of action into the stomach. Obviously, for these gastro-retentive drug forms is necessary keep in consideration the emptying of the stomach. The factors that influence the gastric emptying (hence the retention time) of oral dosage forms are the density, the shape and the dimensions, the simultaneous ingestion of food or drug like anticholinergic and biological factors as age, sex, race, body mass index and presence of pathology [77,78].

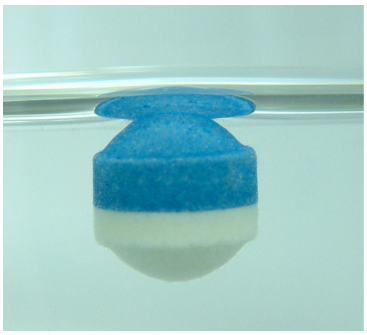

Figure 18: Dome Matrix floating assembled system.

Mixed Configuration

Using both configurations, void and stacked, it possible to obtain a delivery system in which the modules are assembled in mixed configuration (Figure 19).

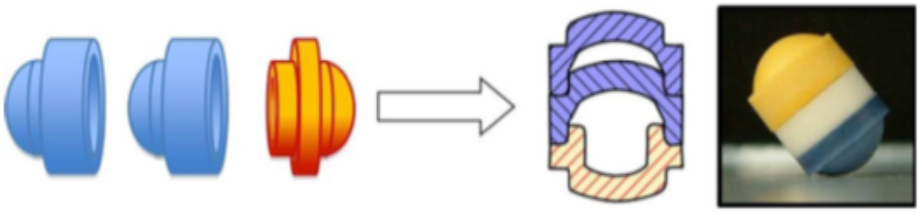

Figure 19: Dome Matrix modules assembled in mixed configuration.

Dome Matrix shows some definite advantages as drug carrier when compared to traditional tablets. For example, in the case of chronic diseases, which require the administration of several medicinal products, the system of issuing Dome Matrix allows to reduce the number of dosage units and to customize therapy, increasing patient compliance.

In dependence on the module assemblage way, different system configurations can be obtained. The modular approach makes possible to administer different drugs at the same time at different rate and in a selected site. Modules of different drug types, doses and release kinetics can be combined in one single

unit. The intended therapeutic regimen and drug release kinetics can be tailored in accordance to the state of diseases and convenience of healthcare/patient management simply by changing the number and type of modules that constitute the system. Modular technology solves the eventual problem of incompatibility between the actives, because each module is individually manufactured by compression and controlled for weight and release.

2. Aim of the work

The purpose of this PhD thesis was the treatment of Benign Prostate Hyperplasia obtained by a dosage form flexible and personalized addressed to the individual needs of every patient. The therapy will be conducted by using two drugs, a 5-phosphodiesterase inhibitor and an alpha lithic, administered in one oral dosage form containing different doses and combination of these two drugs. The development of a single delivery system for oral administration of two drugs was conducted by applying the Dome Matrix technology based on module assemblage for modified release dosage form preparation.

Assembled systems composed by modules containing different doses of silodosin were studied in order to obtain a flexibility of dosage forms. The assembled systems, intended to float, guarantee a prolonged permanence of the dosage form in the stomach. The rationale for the development of sustained release gastro-retentive drug delivery system for this drug is based on the fact that the molecule shows a preferential absorption in the first tract of the intestine, a rapid absorption and a short half-life. Moreover, a sustained release dose of silodosin may reduce its side effects.

They have been prepared modules of silodosin, each containing 2 or 4 mg. In order to obtain a floating system, male and female modules were manufactured. Assembled systems containing 4, 6 and 8 mg, were obtained by assembly two or more modules in void and mixed configurations.The modules were formulated to obtain a sustained release of drug from the gastro-retentive assembled system of approximately 60% in 4 hours and the remaining amount

in the subsequent 2-4 hours. The release of silodosin from the individual modules and the assembled systems was determined by *in vitro* dissolution test in simulated gastric fluid without enzymes at pH 1.2 and dissolution medium at pH 3.5.

The module assembly, at different doses of silodosin, allows customization of the therapeutic dose to be administered to patients.

The combination of silodosin and sildenafil citrate into a single sustained release unit dosage form was also developed. Fixed dose combination products were prepared as sustained drug release dosage forms in order to obtain a prolonged release of the two combined drugs to maintain the drug levels within the therapeutic window and reduce side effects. The assembled system, intended to float for prolonging the time of permanence in the stomach, could improve the bioavailability of the two drugs.

Male and female modules containing silodosin were combined with female and male modules of sildenafil citrate, respectively, in void configuration. The presence of silodosin and sildenafil citrate, each contained in a separate module, should avoid any incompatibility problems.

Since it was observed that the drug release from the module depends on whether the active substance is placed in male or female modules, each drug was formulated in both modules. Therefore, the drug release of assembled systems obtained by the following combinations was investigated:

- male module of silodosin and female module of sildenafil citrate;
- female module of silodosin and male module of sildenafil citrate.

The modules were formulated so as to obtain a sustained release of each drug of approximately 60% after 4 hours.

This part of the doctoral research was carried out at the Department of Pharmacy, University of Parma, while the last part of the PhD thesis was done at the University of Texas at Austin (USA), under the supervision of Professor Nicholas Peppas. The project was focused on the evaluation of swelling behaviour of silodosin and sildenafil citrate individual modules and the related assembled systems. Furthermore, the swelling study of assembled systems of the two drugs was performed using the X-ray computed tomography technique.

3. Materials and Methods

3.1. Materials

The materials used in this PhD research work are the following:

- Silodosin (batch MO130176, Recordati, Milan, Italy)
- Sildenafil Citrate (batch 689620013, Assia Chemical Industries, Teva-Tech, Israel)
- Hydroxypropyl methylcellulose HPMC K15M (batch DT181977, Colorcorn, United Kingdom)
- Hydroxyypropyl methylcellulose HPMC K4M (batch ND30012N01, Colorcorn, United Kingdom)
- Microcrystalline cellulose Avicel PH102 (batch H2692003, ACEF, Piacenza, Italy)
- Mannitol Pearlitol SD200 (batch E556G, Roquette, France)
- β-cyclodextrin (batch E1015, Roquette, France)
- Talc (batch C5239004, Acef, Piacenza, Italy)
- Magnesium Stearate (batch C1402005, Acef, Piacenza, Italy)
- Polyethylene glycol PEG 6000 (batch 1308600, Fluka, Germany)
- Sodium chloride (batch E1336003, ACEF, Piacenza, Italy)
- Potassium phosphate monobasic (batch n. K1191005, ACEF, Piacenza, Italy)
- Sodium dihydrogen phosphate dihydrate (batch G2728001, ACEF, Piacenza, Italy)
- Pepsin, Powder (batch B0140177, Acros Organics, USA)

- Sodium hydroxide drops (batch J1350006, ACEF, Piacenza, Italy)
- Triethylamine (batch STBF4636V, Sigma-Aldrich, USA)

All the used materials and solvents were of analytical grade according the Ph. Eur.

3.2. Methods

3.2.1. Characterization of raw materials

3.2.1.1. Differential Scanning Calorimetry

The thermal behaviour of silodosin and sildenafil citrate was investigated by Differential Scanning Calorimetry (DSC 821e STARe, Mettler Toledo, CH). DSC thermograms were recorded by placing accurately weighed amount of sample (3–10 mg) in a 40 mL aluminum pan, sealed and pierced. The samples were heated at a rate of 5 °C/min from 25 to 250 °C under a flow of dry nitrogen (100 mL/min). The analyses were done in triplicate.

3.2.1.2. X-Ray Powder Diffraction

The solid state of the drugs was also characterized using Powder X-ray Diffraction (PXRD). PXRD diffraction patterns were recorded with a Rigaku MiniFlex diffractometer (Tokyo, J) using a CuKa radiation (30 kV, 15 mA) at a scanning speed of 0.5 angle degree/min with a 2θ scanning range from 2 to 50 angle degree.

3.2.1.3. Laser diffraction particle size analyzer

Laser diffraction is a widely used particle sizing technique for powders characterization in pharmaceutical field. The particle size distribution has a direct influence on material properties such as reactivity or dissolution rate, stability in suspension, efficacy of delivery, texture, appearance, flow ability, handling and porosity.

This technique measure the angular variation in intensity of light scattered as a

laser beam passes through a well dispersed sample. The angular scattering intensity received is then analyzed to calculate the size of the particles responsible for creating the scattering pattern. Large particles scatter light at small angles relative to the laser beam and small particles scatter light at large angles. In laser diffraction a volume distribution, which shows the volume percentage of particles at a given size, is obtained. The particle size is reported as a volume equivalent sphere diameter. This technique provides rapid measurements and repeatability.

Particle size of drug powder was carried out by laser light scattering Spraytec (Malvern Instrument Ltd, UK) equipped with a lens of 300 mm diameter and optical path of 2.5 mm. Approximately 10 mg of the powder was dispersed in cyclohexane and Span 85 0.1% (P/V), sonicated for 10 minutes in water bath and analyzed into a 20 mL cell under magnetic stirring. The study was done in triplicate per each sample.

3.2.1.4. Solubility study in acid environment

The solubility of silodosin and sildenafil citrate in the dissolution media, simulated gastric fluid without enzymes pH 1.2 and in a medium at pH 3.5 (preparation described in section 3.3.12), was determined.

The analysis was conducted using the instrument Shake-Flask (Haake SWB 20, Karlsruhe, Germany). It consists in a water bath, within which a plate, maintained in constant agitation, is housed. Saturated drug solutions in medium at pH 1.2 or at pH 3.5 were prepared. An amount of drug in excess was poured into a 50 mL flask, to which were added 25 mL of fluid. The saturated solutions

were left to condition for 24 hours, immersed in the water bath at 37 °C. Subsequently an aliquot of supernatant was withdrawn from each solution, filtered with cellulose acetate syringe filter of 0.45 μm and analyzed by HPLC, according to the analytical method described in section 3.2.3 and 3.2.4. The analysis was performed in triplicate per each drug.

3.2.2. Stability study in acid environment

Accurately weighed amount of active (about 20 mg of silodosin and 3 mg of sildenafil citrate) were dissolved into a 100 mL volumetric flask with the dissolution medium pH 1.2 or pH 3.5.

Aliquots were collected at time 0 and after 2, 4, 6, 8 and 24 hours, filtered with cellulose acetate syringe filter of 0.45 μm and analyzed by HPLC according to the methods described in section 3.2.3 and 3.2.4. The analysis was performed in triplicate per each of them.

3.2.3. Assay of silodosin content

The quantitative determination of silodosin was carried out by High Performance Liquid Chromatography (HPLC), according to the method developed by Recordati. The HPLC apparatus and the conditions were the following: Shimadzu Liquid Chromatograph LC-10AT (Shimadzu Europe GmbH, Duisburg, Germany); UV-VIS detector SPD-10A at 270 nm; Symmetry C18 column 4.6 mm x 150 mm, 3.5 μm (Waters, Italy), maintained at 40 °C; mobile phase: acetonitrile:phosphate buffer 100 mM (27:73); flow rate: 0.9 mL/min;

injection volume: 10 μL (Autosampler, Waters Corp., Milford, MA, USA); retention time about 6 minutes.

The linearity of the method was verified in the concentration range of 0.001 – 0.1 mg/mL. The system suitability gave the following results: theoretical plates 6724.57; peak symmetry 2; RSD 0.52%.

3.2.4. Assay for sildenafil citrate content

The quantitative determination of sildenafil citrate was carried out by HPLC, following the method reported in USP 35-NF 30. The HPLC apparatus and conditions were the following: Shimadzu Liquid Chromatograph LC-10AT (Shimadzu Europe GmbH, Duisburg, Germany); UV-VIS detector SPD-10A at 290 nm; C18 column 3.9 x 150 mm, 5 um (Waters, Italia), maintained at 30 °C; mobile phase: acetonitrile:methanol:phosphate buffer (17:25:58); flow rate: 1 ml/min; injection volume: 20 μl (Autosampler, Waters Corp., Milford, MA, USA)); retention time about 12 minutes.

The linearity of the method was verified in the concentration range of 0.001 – 0.1 mg/ml. The system suitability gave the following results: theoretical plates 3258.15; peak symmetry 2; RSD 0.76%.

3.2.5. Preparation of wet granulate

In order to ensure uniformity of formulation content and to improve the flow properties during the compression phase, wet granulation of the powders was carried out. The powder blend, consisting of active ingredient and excipients, was mixed in Turbula® (WAB, Basel, Switzerland) for 15 minutes in presence of

one steel ball. Afterwards, the blend was kneaded in a mortar with a binder solution. Granules were obtained by using an oscillating arm granulator (Erweka AR400, Düsseldorf, Germany), equipped with a 0.8 mm mesh. Granules were dried in an oven at 50 ° C for about 5 hours.

3.2.6. Dimensional analysis of granules

The dimensional analysis of the granules was carried out through the use of sieves (Endecotts Limited, London, United Kingdom) placed on sieve shakers (Fritsch GmbH, Idar-Oberstein, Germany) according to the geometric progression of √2 order. The openings of the sieve mesh were the following: 1000, 710, 500, 355, 250, 180 and 125 μm. Prior to analysis each sieve was accurately weighed. To perform the granulometric analysis, the sieves were placed by putting the one with the largest opening on the top and the others in order of decreasing mesh opening up to finish with a round pan, called the receiver. Samples of granules were poured into the top sieve and closed with a lid. Then, the stack of sieves were subjected to vibrations for 5 minutes at amplitude 4. The sieves were weighed and placed on the sieve shakers for additional 5 minutes at amplitude 4. The sieves were weighed again. Knowing the opening of each mesh sieve, the size class of the particles corresponding to the fraction collected on the sieve is equal to the arithmetic mean between the opening of the above sieve and that of the below one. The fractions collected on each sieve were weighed and the amount of granules for each size fraction was expressed as the percentage fraction of the weight of granulate analyzed.

3.2.7. Bulk and Tapped density of granulate

The bulk density of a powder is defined as the mass of particles divided by the total volume occupied. The total volume includes particle volume, interparticle void volume, and internal pore volume. The bulk density of a powder is the ratio of the mass of an untapped powder sample to its volume including the contribution of the interparticulate void volume. Bulk density is not an intrinsic property of a material; it can change depending on how the material is handled. Hence, it depends on both the density of powder particles and the spatial arrangement of particles in the powder bed. The bulk density is expressed in gram per millilitre (g/mL). The measurement of the bulk density was carried out by pouring a known quantity of granules (about 2 g) in a 10 mL graduated cylinder and measuring the volume occupied by the granulated. The apparent density was then calculated from the ratio between the weight of the powder poured (expressed in grams) and the occupied volume (expressed in mL).

The tapped density is as an increased bulk density attained after mechanically tapping a container containing the powder sample. The tapped density is obtained by mechanically tapping a graduated measuring cylinder or vessel containing the powder sample. After observing the initial powder volume or mass, the measuring cylinder or vessel is mechanically tapped, and volume or mass readings are taken until little further volume or mass change is observed. The mechanical tapping is achieved by raising the cylinder or vessel and allowing it to drop, under its own mass, a specified distance.

Measuring density after settling (Tapped Density) was carried out using the

instrument Tapped Density Tester (Erweka GmbH, Heusenstamm, Germany). A known amount of powder (approximately 2 grams) was poured, avoiding the packing, in a 10 mL graduated cylinder attached to the instrument. After secure the graduated cylinder on a support, it was then subjected to cycles of 50, 500 and 1250 taps. After each interval of taps the volume occupied by the powder was measured. If after 1250 taps a change in powder powder was observed with respect to the previous cycle, the powder was subjected to a further cycle of 1250 taps. The density after settling of the granulated is calculated from the ratio between the weights of the granulated poured (grams) and the volume occupied after 1250 taps.

3.2.8. Manufacture of Dome Matrix modules

The blend for the manufacturing of Dome Matrix modules were prepared by mixing the granulated with 1% (w/w) of magnesium stearate and 3% (w/w) of talc in a Turbula® (WAB, Basel, Switzerland) for 5 minutes. Dome Matrix modules were obtained using an alternating tableting machine (KORSH, Mod. 9341-72, Berlin) equipped with special punches of 7.5 mm diameter (Figures 20 and 21).

(a) (b)

Figure 20. Images of the upper female punches (a) and the upper male punches (b).

(a) (b)

Figure 21. Combinations of dies and lower punches (7.5 mm diameter) for the manufacturing of (a) stackable modules and (b) terminal modules.

- Terminal female modules: obtained with fixed die and 7.5 mm diameter punch (Figure 21 (b)), characterized by a 1.4 mm curvature with round terminal base for the lower punch and by a particular convex base for the upper punch that enables the interlocking with the male module.
- Stackable female modules: obtained with adjustable die and 7.5 mm diameter punch (Figure 21 (a)). The lower punch has a special geometry that, together with the adjustable die, allows the formation of a groove on the edge of the convex base of the module, to make possible its assemblage with an other female module (stackable or terminal) to obtain piled configuration. The upper punch is the same used for terminal female modules.
- Terminal male modules: obtained with fixed matrix and 7.5 mm diameter punches, characterized by a round terminal base with curvature of 1.4

mm for the lower punch and by a special shape for the upper punch which allows for the formation of annular protrusion.

- Stackable male modules: obtained with adjustable die and 7.5 mm diameter punches. The lower punch is the same used for the manufactuting of stackable female modules, while the upper punch is the same used for terminal male modules.

The peculiar geometry of the release modules has been designed to allow modules to be assembled in different configurations to create various systems of drug release. The assembled systems were obtained by friction interlocking of the modules.

The Dome Matrix modules were measured in terms of height, diameter, thickness, concavity depth in addition to the annular protrusion diameter of the male module. A caliber (Absolute Digimatic Caliber, Mitutoyo Corporation, Japan) and thickness gage (Absolute Digimatic Thickness, Mitutoyo Corporation, Japan) were used.

3.2.9. Friability test

The measure of tablets friability was carried out according to the method reported in the Ph. Eur. 8th ed., using the friability tester Roche (Erweka® GmbH, Düsseldorf, Germany). A rolling drum of transparent synthetic polymer, having diameter of 30 cm and thickness of 4 cm, was used. One side of the drum is removable. The modules were tumbled at each turn of the drum by a curve projection that extends from the middle of the drum to the outer wall. The drum is attached to the horizontal axis of a device that rotates at 25±1 rpm.

Thus, at each turn the modules roll or slide and fall onto the drum wall or onto each other. Ten modules for each formulation (female and male modules) were carefully dusted and weighed on an analytical balance. The modules were then placed into the drum of the friability test apparatus and the drum was rotated for 4 minutes; at the end the modules were dusted again before weighing.

Friability is defined as the percentage of the weight loss by the tablets due to mechanical action during rolling. Friability is expressed as a percentage loss on the module weight according to the equation 3.

$$\text{Friability}\ (\%) = \frac{W_1 - W_2}{W_1} * 100 \qquad \text{(eq. 3)}$$

where W_1 is the weight of the module before the analysis and W_2 is the weight of the module after the friability test. The loss in weight should not be greater than 1% of the initial module weight.

3.2.10. Measurement of the hardness of the tablets

The measurement of hardness was carried out according to the procedure reported in Ph. Eur 8th ed., using the Monsanto apparatus. The device consists of two opposed clamps, one of which moves to the other. The mobile support is connected to a spring on which it is possible to exert pressure through a rotating screw. The flat surfaces of the clamps are perpendicular to the direction of movement. The module is firmly fixed to the surface of the clamps, which has to be flat and wider than the area of contact with the module. The modules were placed in two directions as it is shown in Figure 22. The number of the modules per batch that were tested was ten (five in one position and five in the other). The results, according to Ph. Eur 8th Ed., were expressed as mean of minimum

and maximum forces measured in Kilograms.

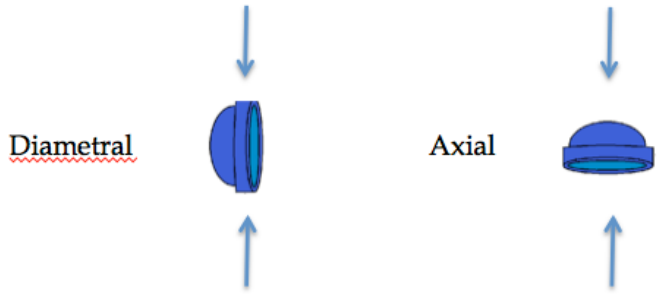

Figure 22. Positions of modules tested with Monsanto device.

3.2.11. Analysis of drug content in the modules

Five tablets per each batch was weighted and then crushed in a mortar; three samples of powder (about the mean weight of the 5 tablets) were collected. The samples were put in a 200 mL volumetric flask with the dissolution medium (described in section 3.2.12) and stirred with magnetic bar for 5 hours. The samples were filtered using cellulose acetate filter (cut-off 0.45 μm) and then analyzed by HPLC.

3.2.12. *In vitro* dissolution test

The *in vitro* dissolution studies were performed using dissolution apparatus II (USP 38 Ed.). The dissolution tester (Agilent VK-7025, Weston Parkway, Cary, NC, USA) was equipped with paddle, operated at a speed of 50 rpm. The dissolution tests were performed in simulated gastric fluid without enzymes at pH 1.2 and at pH 3.5, heated at 37 ± 0.5 °C. The simulated gastric fluid was prepared dissolving 2 g of sodium chloride and 7 mL of hydrochloric acid 37%

in one liter of deionized and degassed water; the pH was adjusted with sodium hydroxide or hydrochloric acid to obtain the value at 1.2. The dissolution medium at pH 3.5 was prepared dissolving 6.8 g of potassium dihydrogen phosphate in one liter of deionized and degassed water. The pH was adjusted with hydrochloric acid until the value of 3.5.

In each vessel containing 900 mL of dissolution medium was introduced a Dome Matrix module. Aliquots of 1.5 mL dissolution medium were collected at fixed time points (15, 30, 60, 120, 180, 240, 300 and 360 minutes) from each vessel with an auto-sampler (Agilent 8000, Weston Parkway, Cary, NC, USA) and subsequently analyzed by HPLC (as described in assay method section 3.2.3 and 3.2.4).

The *in vitro* dissolution test was carried out on triplicate for each module type and assembled system. In some cases, the *in vitro* dissolution tests were carried out by placing the modules or the assembled system in sinker (USP 38).

3.2.13. Similarity factor

The dissolution profiles were compared using a model independent method through a similarity factor f_2, which is a logarithmic reciprocal square root transformation of the sum of the squared error and is a measurement of the similarity in the percent (%) dissolution between the two curves.

The dissolution profiles were compared through the similarity factor f_2 calculated by the equation 4:

$$f_2 = 50 * \log\left\{\left[1 + \left(\frac{1}{n}\right)\sum_{t=1}^{n}(R_t - T_t)^2\right]^{0.5} * 100\right\} \qquad \text{(eq. 4)}$$

where n is the number of dissolution sample time, R_t and T_t represent the mean

percent drug released at each time point *t* for the reference and the test products, respectively.

For curves to be considered similar, f_2 values should be close to 100. Generally, f_2 values greater than 50 (50-100) ensure that the profiles are similar.

This independent method is most suitable for dissolution profile comparison when three to four or more dissolution time points are available. As further suggestions for the general approach, the following conditions should also be considered:

- The *in vitro* dissolution of the test and reference products should be made under exactly the same conditions. The dissolution time points for both the profiles should be the same (e.g., 15, 30, 45, 60 minutes). The reference batch used should be the most recently manufactured prechange product.
- Only one measurement should be considered after 85% dissolution of both the products.
- Because the data are used, the percent coefficient of variation at the earlier time points (e.g., 15 minutes) should not be more than 20%, and at other time points should not be more than 10%.

3.2.14. Swelling studies

Swelling is referred to the growth in size of the module due to the water uptake of water and formation of polymer gel.

Analysis of the dynamic swelling behavior of the Dome Matrix modules was performed in four different media: simulated gastric fluid without enzymes at pH

1.2 (as described in the section 3.2.12), simulated gastric fluid with enzymes pH 1.2, pH 3.5 (as described in the section 3.2.12) and simulated intestinal fluid without enzymes at pH 6.8. The simulated gastric fluid with enzymes was prepared dissolving 2 g of sodium chloride and 3.2 g of purified pepsin and 7 mL of hydrochloric acid 37% in one liter of deionized and degassed water. The pH was adjusted with sodium hydroxide or hydrochloric acid until the value of pH 1.2 ± 0.1.

The simulated intestinal fluid without enzyme at pH 6.8 was prepared by dissolving 6.8 g of monobasic potassium phosphate in 250 mL of deionized water and then adding 77 mL of 0.2 N sodium hydroxide and 500 mL of water. The resulting solution was adjusted with 0.2 N sodium hydroxide or 0.2 N hydrochloric acid to a pH of 6.8 ± 0.1 and finally diluted to 1000 mL.

The medium was placed in a glass bottle and heated at 37 ± 0.5 °C in a thermostatic bath (Shaking water bath, VWR, Radnor, PA, USA).

The modules were weighed before swelling process and then putted in 100 mL of medium. At the same time, a stopwatch was initiated to record the swelling time of the sample. After a definite swelling time the sample was removed from the solution and the surface water was quickly removed with a filter paper. The sample was weighed. The swelling studies, conducted on Dome Matrix modules, were performed in a time interval of 8 hours.

The modules were removed and weighted at fixed time points (15, 30, 60, 120, 180, 240, 300, 360, 420 and 480 minutes).

The weight swelling ratio (q) at different time can be calculated using the equation 5:

$$\text{Weight Swelling Ratio (q)} = \frac{W_{wet}}{W_{dry}} \qquad \text{(eq. 5)}$$

where W_{dry} is the weight of dry module before testing and W_{wet} is the weight of module after their immersion in a test solution.

3.2.15. High-resolution X-ray computed tomography studies

X-ray Computed Tomography (X-ray CT) is a nondestructive technique for visualizing interior features within solid objects, and for obtaining digital information on their 3-D geometry and properties. This technique has been widely used for the *in vivo* imaging of plants, insects, animals, and humans. X-ray tomography is a relatively new approach to imaging the internal structure of solid dosage forms. This technique has high penetration ability and provides a reasonable level of resolution. A CT scan, also called computerized axial tomography scan (CAT scan), makes use of computer-processed combinations of many X-ray images taken from different angles to produce cross-sectional (tomographic) images (virtual 'slices') of specific areas of a scanned object, allowing the user to see inside the object without cutting.

The simplest common elements of X-ray radiography are an X-ray source, an object to be imaged through which the X-rays pass, and a series of detectors that measure the extent to which the X-ray signal has been attenuated by the object (Figure 23). A single set of X-ray intensity measurements on all detectors for a given object position and scanner geometry is termed a view. The fundamental principle behind computed tomography is to acquire multiple views of an object over a range of angular orientations. By this means, additional

dimensional data are obtained in comparison to conventional X-radiography, in which there is only one view.

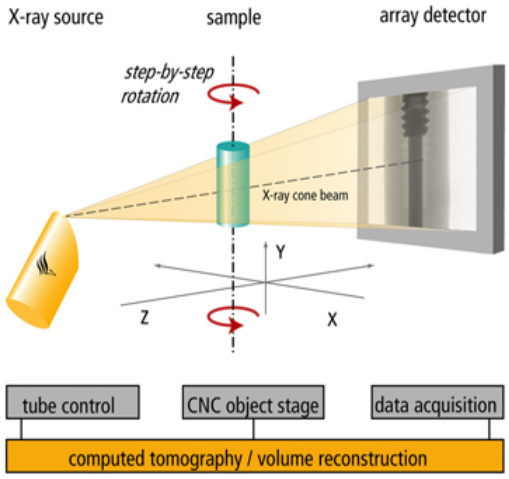

Figure 23. Schematic diagrams of X-ray CT.

The CT experiments were carried out at the High-resolution X-ray CT Facility in the Department of Geological Sciences at the University of Texas at Austin. This non-destructive, high-resolution visualization with X-ray CT was used to follow the process of swelling and dissolution of the swellable Dome Matrix modules.

During the experiments each assembled system was placed in a test tube in which a polymer support foam was placed on the bottom to hold up the specimen, since it cannot be moved during the scan. The test tube was filled with Simulated Gastric Fluid at pH 1.2 (preparation described in section X) at room temperature. The test tube was kept vertically.

In the case of the floating system, the assembly was put in the test tube filled with the fluid and a funnel was put on the top to keep it stable. Using an 18.9 μm resolution and an average scanning time of 5 minutes, data were collected

for these swellable matrices in the dry state and at 15, 30, 45, 60, 120 and 180 minutes. Calibration was necessary to establish the characteristics of the X-ray signal as read by the detector. CT data were then collected and special software was required to reconstruct the raw CT images. In particular, Avizo ver.9.1 software (FEI company, Hillsboro, Oregon, USA) was used to obtain three-dimensional image data.

4. Results and Discussion

4.1. Characterization of silodosin raw material

The active substance silodosin was characterised in terms of particle size distribution and solid state analyses.

The particle size measurement of the powder was carried out by laser light scattering Spraytec. The dimensional analysis of silodosin (Figure 24) showed a monodimensional distribution with Dv_{50} equal to 3.62 ± 0.34.

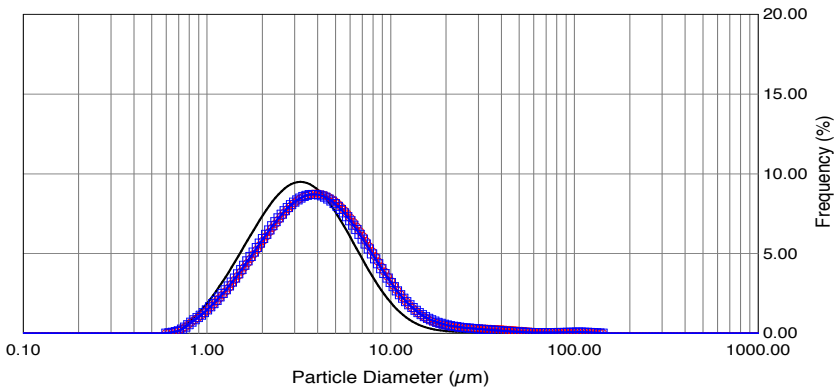

Figure 24. Dimensional distribution of silodosin powder.

The X-ray analysis of silodosin powder evidenced the presence of diffraction peaks, typical of drug crystalline structure (Figure 25).

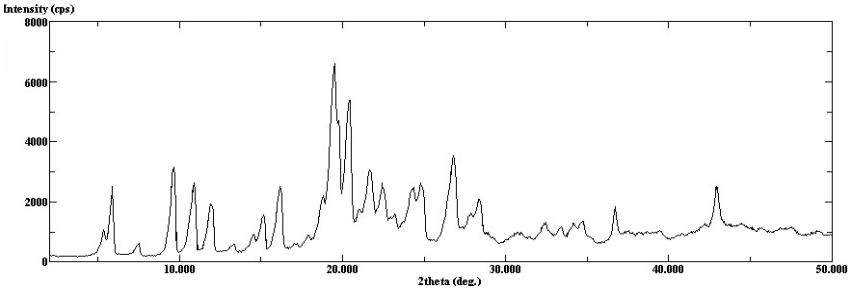

Figure 25. X-ray spectra of silodosin powder.

The DSC thermogram (Figure 26) showed the presence of an endothermic peak at 107 °C corresponding to melting point of silodosin, in accordance with the analysis certificate.

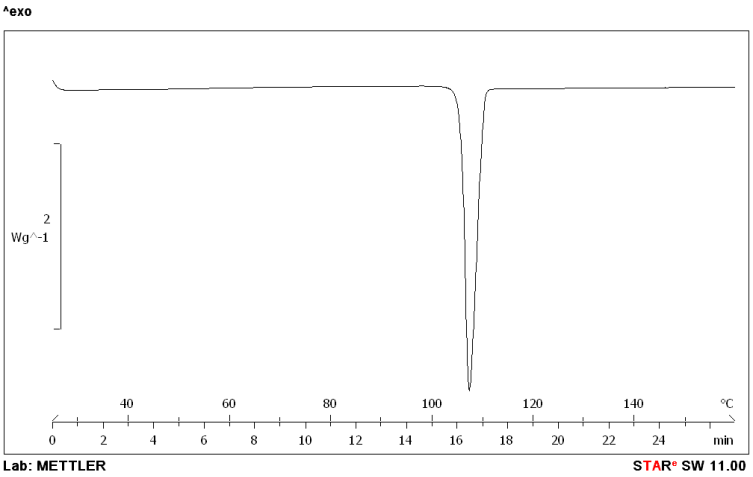

Figure 26. DSC curve of silodosin powder.

Table I shows the solubility values of silodosin at pH 1.2 and pH 3.5 at 37 ± 0.5 °C. As can be observed from the values, the solubility of silodosin decreases as the pH increases.

Table I. Solubility of silodosin at 37 ± 0.5 °C

Solubility	mg/mL
pH 1.2	34.70 ± 0.95
pH 3.5	13.44 ± 0.11

4.2. Validation of the HPLC method for the silodosin assay

The HPLC method for the analysis of silodosin was validated according to the Ph. Eur. 8th Ed., considering the following parameters:

- Linearity: the linear relationship between the chromatogram signals and the analyte concentrations by applying linear regression equation (Figure 27). The linear regression coefficient r^2 for silodosin was 0.99996.

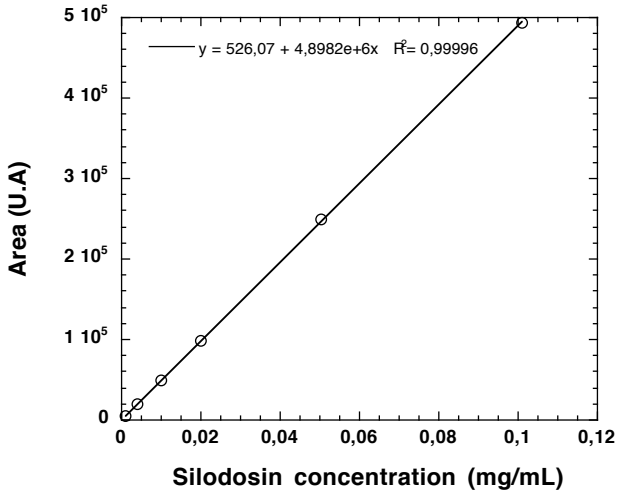

Figure 27. Area of chromatographic peaks obtained from silodosin solutions plotted vs their concentration.

- Theoretical plates: calculated using the following formula

$$N = \frac{t}{W^2}$$

where t indicates the retention time and W the width of the base of the peak. The number of theoretical plates (N) for silodosin was 6724.57 ± 404.17.

- Tailing factor: calculated using the following formula

$$T = \frac{W_{0.05}}{2f}$$

where $W_{0.05}$ indicates the peak width at 1/20 of its height, while f represents the distance between the perpendicular drawn from the maximum peak and the start point of the peak at 1/20 of its height.

The tailing factor for silodosin was 2.

4.3. Manufacturing of silodosin controlled release module

Modules of silodosin, containing 2 or 4 mg, were manufactured to be assembled in order to obtain a dosage form flexible and customizable using the Dome Matrix technology.

4.3.1. Silodosin 4 mg module

Due to the low drug dose, in order to avoid an uneven distribution of silodosin in the formulation for the manufacturing of 4 mg module, wet granulation of silodosin and excipients was carried out.

Silodosin was granulated with the components reported in Table II, except for talc and magnesium stearate that were added extra-granular. As binder solution 7.5 mL of an aqueous solution containing 10% (w/v) PEG 6000 were used. The granules were dried in oven for 5 hours at 50 °C.

Table II. Composition of silodosin 4 mg F#A module.

Components	Weight (mg)	Percentage (w/w)
Silodosin	4.00	2.6
Avicel PH102	68.92	45.2
Methocel K15M	33.14	21.7
Pearlitol 200 SD	33.14	21.7
PEG 6000	7.50	4.9
Talc	4.40	2.9
Magnesium stearate	1.47	1.0
Total	**152.57**	**100**

The manufacturing of the terminal female modules was easily obtained, while the terminal male modules were more difficult to manufactured due to the fracture of the annular protrusion.

Before carrying out the *in vitro* dissolution tests, the stability of the drug in the media used (pH 1.2 or pH 3.5) was investigated. The HPLC analysis did not show the presence of other chromatographic peaks apart that corresponding to silodosin; no significant decrease in the drug amount (%) was observed (Figure 28).

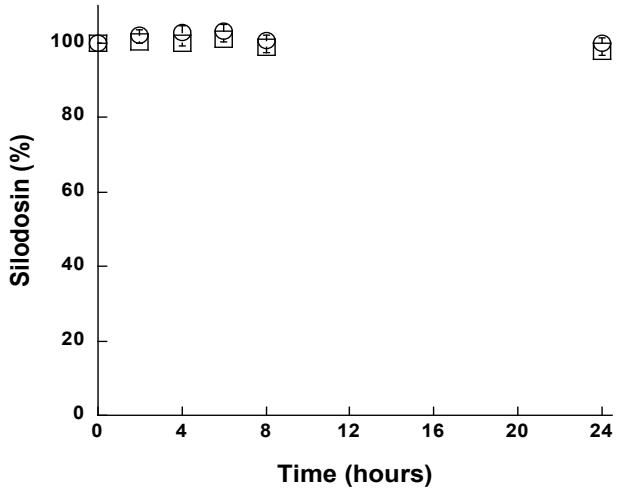

Figure 28. Stability of silodosin at pH 1.2 (○) and pH 3.5 (□) (mean ± standard deviation, n = 3).

The *in vitro* dissolution test of female and male modules was carried out at pH 1.2. The dissolution profiles, reported in Figure 29, showed for both types of modules a prolonged release. After 4 hours the amount of silodosin released was higher than 80%.

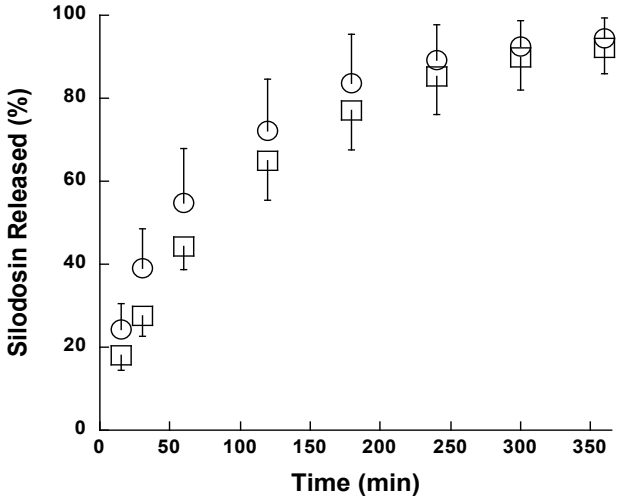

Figure 29. Release profile of silodosin 4 mg F#A at pH 1.2 (O) female module and (□) male module (mean ± standard deviation, n = 3).

As can be noticed from the graph in Figure 29, the silodosin release from the female module was higher than that from the male module. This behaviour is due to the greater surface area in the female module with respect to the male module attributed to their peculiar shape.

In order to improve the granulate cohesion and the compression process of the male module, PEG 6000 was added as a powder during the wet granulation and the amount of Avicel was reduced. As binder solution, 5 mL of deionized water were used. The composition of modules is summarised in Table III. Both female and male modules of silodosin 4 mg F#B were easily manufactured.

Table III. Composition of silodosin 4 mg F#B module.

Components	Weight (mg)	Percentage (w/w)
Silodosin	4.00	3.6
Avicel PH102	33.14	29.4
Methocel K15M	33.14	29.4
Pearlitol 200 SD	33.14	29.4
PEG 6000	5	4.3
Talc	3.24	2.9
Magnesium stearate	1.08	1.0
Total	**112.74**	**100**

During the *in vitro* dissolution test the modules behaved differently: all male modules were positioned on the bottom of the vessel, some female modules floated and others sunk on the bottom of the vessel. This behaviour affected the drug release of the drug since a surface portion of the floating female modules was not exposed to the dissolution medium. Besides, the modules that sank to the bottom of the vessel often stuck to it, in this way a portion of the release surface was hidden.

To prevent these problems it was decided to conduct the dissolution test by placing the modules in sinkers (USP 34), perforated stainless steel cylinders. In this way all the faces of the modules were exposed to the dissolution medium. The dissolution profiles at pH 1.2 of silodosin 4 mg from the male and female modules, placed individually in the sinker, are illustrated in Figure 30. About 100% drug release from the individual modules was obtained after 6 hours.

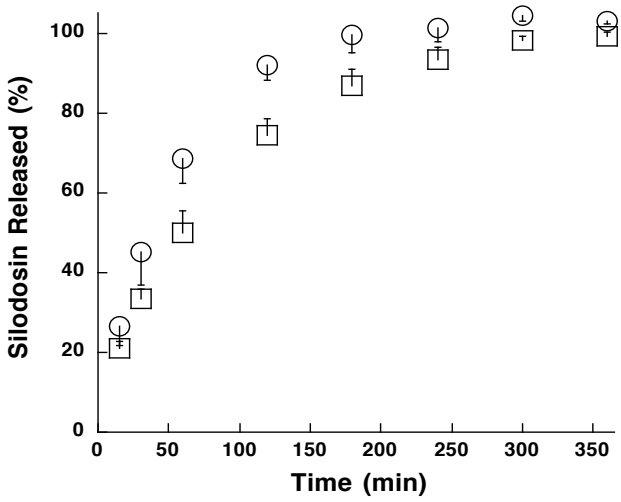

Figure 30. Release profile of silodosin 4 mg F#B at pH 1.2 in sinker (○) female module and (□) male module (mean ± standard deviation, n = 3).

Also the dissolution test of male and female modules of silodosin 4 mg at pH 3.5 was carried out in sinker. Figure 31 shows the dissolution profiles. After 4 hours the amount of drug released from both modules was comparable with the drug released at pH 1.2. However, the drug release was slower at the beginning of dissolution at pH 3.5 due to the lower silodosin solubility at this pH value (see Table I).

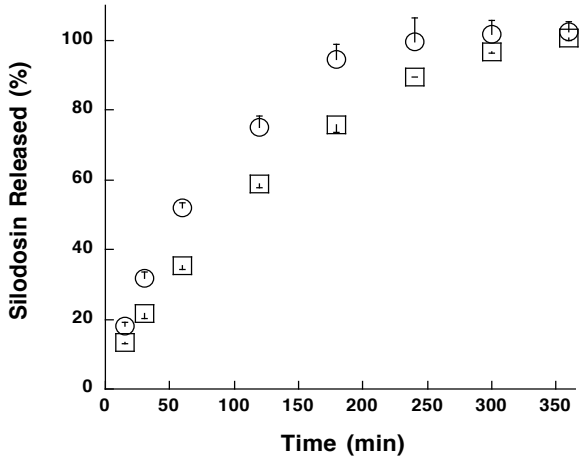

Figure 31. Release profile of silodosin 4 mg F#B at pH 3.5 in sinker (○) female module and (□) male module (mean ± standard deviation, n = 3).

It is important to underline that the silodosin 4 mg modules did not disintegrate at pH 1.2 and at pH 3.5.

The granulate of silodosin 4 mg F#B was then characterized. The analysis of size distribution of silodosin granulate, performed with the sieve test, is showed in Figure 32. As can be observed from the graph, the dimensions of the granules were mainly distributed between 355 and 710 µm.

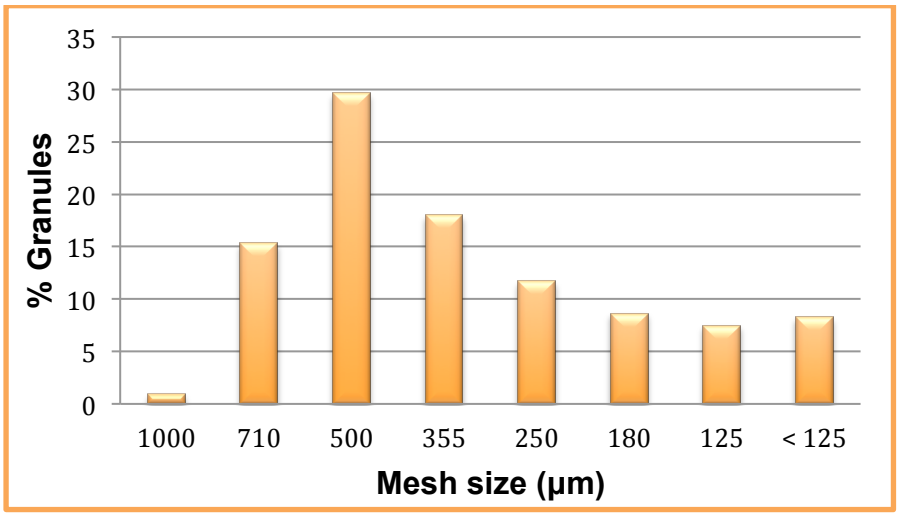

Figure 32. Dimensional distribution of silodosin 4 mg F#B granules.

The granulate of silodosin was also characterised in terms of residual moisture content, tapped density and bulk density.

The residual moisture content, determined with a volumetric titration, showed a value of 4.95 ± 0.21% (w/w). The results of bulk density test showed a value of 0.26 g/mL, while the tapped density was 0.34 g/mL.

The silodosin modules F#B were characterised in terms of weight, height and diameter (Table IV).

Table IV. Values of weight, height and diameter of male and female terminal modules of silodosin 4 mg (mean ± standard deviation, n = 10).

	Weight (mg)	Height (mm)	Diameter (mm)
Terminal Female	111.7 ± 3.8	4.23 ± 0.09	7.56 ± 0.02
Terminal Male	113.0 ± 5.2	3.68 ± 0.10	7.52 ± 0.01

The male and female modules showed a friability value of 0.18% and 0.27% respectively, according to the specifications of Ph. Eur. 8th Ed. The values of the hardness of the modules, in both diametral and axial orientations, are summarized in Table V.

Table V. Hardness of the terminal male and female modules of silodosin 4 mg F#B.

	Diametral (N)	Axial (N)
Terminal Female	28.45 ± 2.16	44.14 ± 5.98
Terminal Male	44.15 ± 7.75	54.94 ± 8.73

Diametral hardness is lower than axial because the lateral side of the module is thinner and less compressed than the dome, because of the peculiar shape of the module.

4.3.2. Silodosin 2 mg module

Silodosin was wet granulated with the excipients reported in Table VI except for talc and magnesium stearate, which were added extra-granular. As binder solution 4 mL of deionized water were used. Female and male modules, both terminal and stackable, of silodosin 2 mg F#A were manufactured.

Table VI. Composition of silodosin 2 mg F#A module.

Components	Weight (mg)	Percentage (w/w)
Silodosin	2.00	1.7
Avicel PH102	34.14	30.3
Methocel K15M	33.14	29.4
Pearlitol 200 SD	34.14	30.3
PEG 6000	5.00	4.4
Talc	3.24	2.9
Magnesium stearate	1.08	1.0
Total	**112.74**	**100**

The dissolution profiles of silodosin 2 mg female and male modules in sinker at pH 1.2 are illustrated in Figure 33. After 6 hours 100% drug release from both individual modules was achieved.

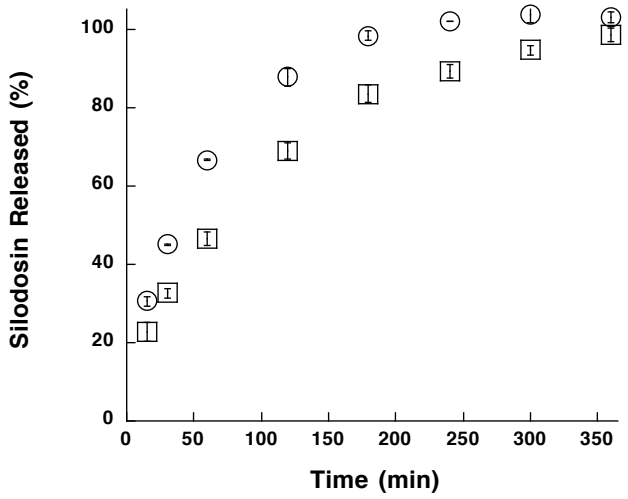

Figure 33. Release profile of silodosin 2 mg at pH 1.2 in sinker (○) female module and (□) male module (mean ± standard deviation, n = 3).

As previously noticed for the 4 mg silodosin modules, at pH 3.5 (Figure 34) the drug release is slower with respect of that showed at pH 1.2 due to the lower solubility of silodosin at higher pH value. No disintegration of silodosin 2 mg modules at pH 1.2 and at pH 3.5 was observed.

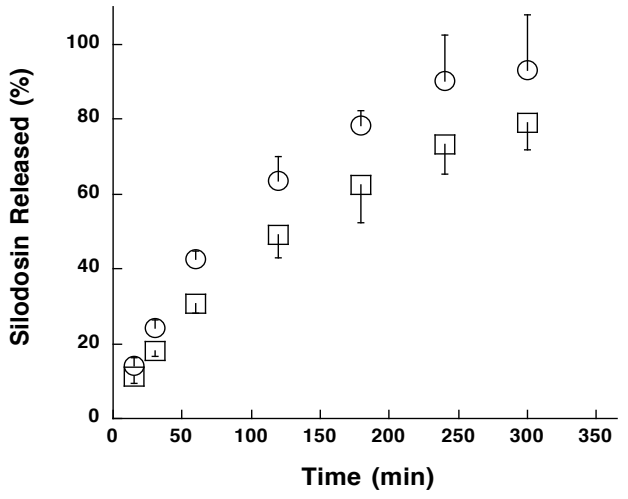

Figure 34. Release profiles of silodosin at pH 3.5 in sinker (○) female module and (□) male module (□) (mean ± standard deviation, n = 3).

The granulate of silodosin 2 mg F#A was then characterized.

The analysis of the size distribution of silodosin 2 mg granules, performed with the sieve test, is showed in Figure 35. As can be observed from the graph, the granules were mainly distributed between 500 and 710 µm.

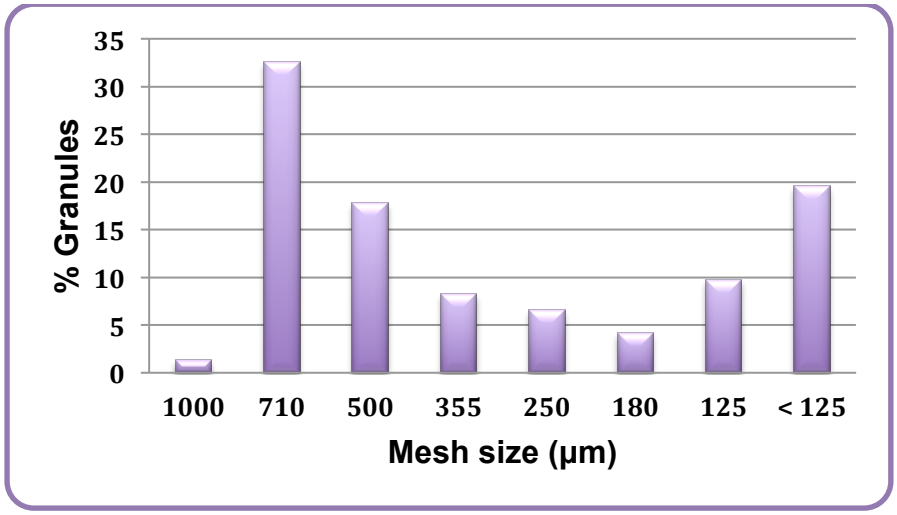

Figure 35. Dimensional distribution of silodosin 2 mg F#A granules.

The granulate of silodosin F#A was also characterized in terms of residual moisture content, tapped density and bulk density.

The residual moisture content, determined with a volumetric titration, showed a value of 2.49 ± 0.22% (w/w). The results of bulk density test showed a value of 0.25 g/mL, while the tapped density was 0.38 g/mL.

The 2 mg silodosin modules were characterised in terms of weight, height and diameter (Table VII).

Table VII. Values of weight, height and diameter of silodosin 2 mg F#A modules (mean ± standard deviation).

	Weight (mg)	Thickness (mm)	Diameter (mm)
Terminal Female	111.6 ± 4.7	4.21 ± 0.08	7.55 ± 0.01
Terminal Male	111.4 ± 2.5	4.40 ± 0.06	7.55 ± 0.02
Stackable Female	111.7 ± 3.4	3.63 ± 0.05	7.51 ± 0.05
Stackable Male	113.5 ± 2.9	3.88 ± 0.05	7.54 ± 0.02

The male and female terminal modules showed a friability value of 0.18%, while the male and female stackable modules showed a value of 0.09%, according to the specifications of Ph. Eur. 8th Ed. The values of the hardness of the modules, in both diametral and axial orientations, are summarized in Table VIII.

Table VIII. Hardness of male and female modules of silodosin 2 mg F#A.

	Diametral (N)	Axial (N)
Terminal Female	27.48 ± 4.41	39.23 ± 11.97
Terminal Male	43.15 ± 6.37	65.70 ± 15.40
Stackable Female	22.56 ± 5.59	40.21 ± 8.73
Stackable Male	41.19 ± 7.45	64.72 ± 6.37

As in the case of silodosin 4 mg F#B modules the diametral hardness is lower than axial because the side of the module is thinner and less compressed than the dome.

4.3.3. Assembled system of silodosin module with placebo module

Since the silodosin modules were intended to be assembled, the surface of the system exposed to the dissolution medium changed respect to the individual modules. In order to investigate if the assemblage of the modules affected the drug release, placebo modules were manufactured to be combined with a silodosin module in void configuration.

The placebo modules were manufactured using the formulation reported in Table IX.

Table IX. Composition of placebo blend.

Components	Weight (mg)	Percentage (w/w)
Avicel PH102	67.2	60
Methocel K4M	33.6	30
Talc	5.6	5
Magnesium stearate	4.5	4
Yellow Lake	1.1	1
Total	**112.0**	**100**

The silodosin female or male modules were assembled in void configuration, respectively, with male or female placebo modules.

4.3.4. Assembled system of silodosin 4 mg F#B module with placebo module

The silodosin release profiles of the assembled systems at pH 1.2 are illustrated in Figure 36. The assembled systems floated immediately when immersed in the dissolution medium and the floatation lasted throughout the dissolution time. No disintegration was observed. The release of silodosin from the female module, combined with the placebo male module, after 4 hours was about 83% while the drug release from the individual female module was about 100% (see Figure 30). The release of silodosin from the male module, combined with a placebo female module, was about 75% after 4 hours while the release from the individual male module was about 93%. The decrease of the silodosin release from the assembled system, compared to the individual modules, was due to the decrease of the surface area exposed to the dissolution medium as the concave bases are not in contact with the fluid.

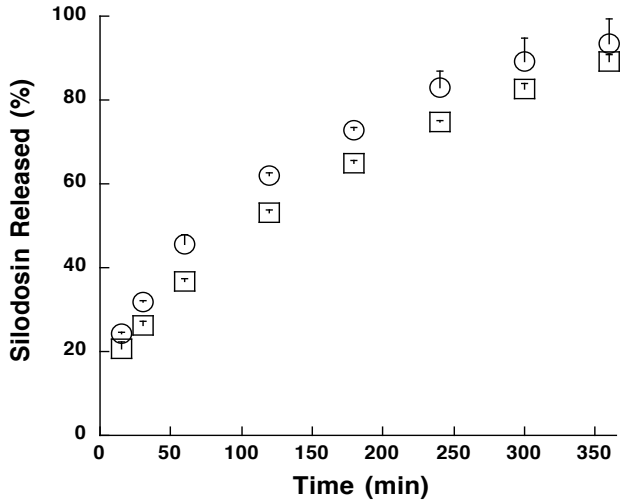

Figure 36. Release profiles of silodosin at pH 1.2 from the assembled system in void configuration: (○) silodosin 4 mg female module/placebo male module and (□) silodosin 4 mg male module/placebo female module (mean values ± standard deviations, n = 3).

The release profiles of the assembled systems at pH 3.5 are showed in Figure 37. Also in this case, the assembled systems floated immediately when immersed in the dissolution medium and the floatation lasted throughout the dissolution time. No disintegration was observed. The release of silodosin from the female module combined with the placebo male module after 4 hours was about 53% while the release from the individual female module was about 100% (see Figure 31). The release of silodosin from the male module combined with a placebo female module was about 55% after 4 hours while the release from the individual male module was about 90%.

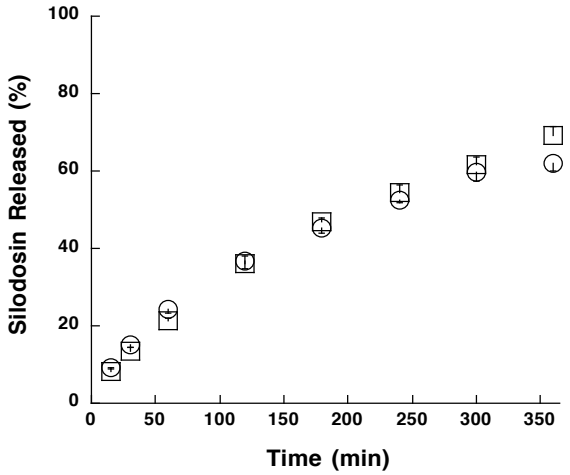

Figure 37. Release profiles of silodosin at pH 3.5 from the assembled system in void configuration: (○) silodosin 4 mg female module/placebo male module (□) and silodosin 4 mg male module/placebo female module (mean values ± standard deviations, n = 3).

In summary, the release of silodosin at pH 1.2 from the modules assembled with the placebo modules decreased about 20% respect to the individual modules. At pH 3.5, the release of silodosin from the assembled systems decreased about 40%. However, the aim to obtain at pH 1.2 an in vitro drug release of at least 60% in 4 hours was achieved.

4.3.5. Assembled system of silodosin 2 mg F#A module with placebo module

One male or female module of silodosin 2 mg was assembled in the void configuration with the corresponding female or male placebo module.

The *in vitro* dissolution tests were performed at pH 1.2 and pH 3.5.

The assembled systems floated immediately when immersed in the dissolution medium and the floatation lasted throughout the dissolution time. No disintegration was observed.

The release profiles of the assembled systems at pH 1.2 are reported in Figure 38. The release of silodosin after 4 hours from the female module combined with the placebo male module was about 60%, while from the individual female module was 100% (Figure 33). The release of silodosin from the male module combined with the female placebo module was 56%, while from the individual male module was 89%.

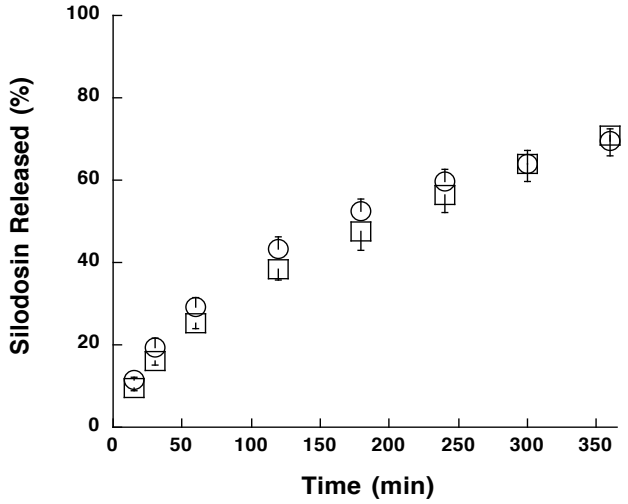

Figure 38. Release profiles of silodosin at pH 1.2 from the assembled system in void configuration: (○) silodosin 2 mg female module/placebo male module and (□) silodosin 2 mg male module/placebo female module (mean values ± standard deviations, n = 3).

The release profiles of the assembled systems at pH 3.5 are reported in Figure 39. The release of silodosin after 4 hours from the female module combined with the male placebo module was about 58%, while from the individual female module was 90% (Figure 34). The release from the male module combined with the female placebo module was 51%, while from the individual male module was 73%.

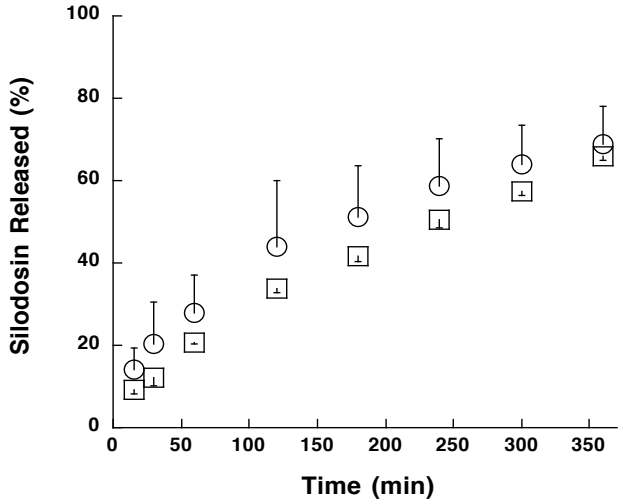

Figure 39. Release profiles of silodosin at pH 3.5 from the assembled system in void configuration: (○) silodosin 2 mg F#A female module/placebo male module and (□) silodosin 2 mg F#A male module/placebo female module (mean values ± standard deviations, n = 3).

In summary, it was observed that the release at pH 1.2 by the individual modules compared to the assembled systems decreased about 40%. At pH 3.5 the decrease of the release from the individual modules compared to the assembled system was approximately 35%. The decrease of drug release was due the different surface area available when two modules were combined together to obtain the assembled system.

Moreover, the decreased drug release rate from the silodosin 2 mg module, assembled with the placebo module, with respect to the silodosin 4 mg module,

assembled with the placebo module, is probably due to the different drug/HPMC ratio (w/w) in the two formulations.

4.3.6. Assembled system in void configuration containing 8 mg of silodosin

Male and female nodules, containing both 4 mg of silodosin, were combined in void configuration to obtain an assembled system of 8 mg.

During the in vitro dissolution the assembled systems floated. As a portion of the assembled systems was not in contact with the dissolution medium, in order to verify if this could affect the drug release the dissolution tests were also performed by placing the assembled systems in sinkers.

In the case of the in vitro dissolution without sinker, all the assembled systems floated immediately when immersed in the medium and the floatation lasted throughout the experiment. In contrast, when the assembled systems were placed in the sinkers, they settled on the bottom of the vessels during the dissolution.

The release of silodosin from the floating system at pH 1.2 after 4 hours was about 63%, while the drug release from the assembled system placed in the sinker was about 77% (Figure 40). The increase percentage of drug release was due to the fact that using the sinkers the entire surface of the assembled system was in contact with the medium, while in absence of sinker the assembled system floated and then a portion of the surface was not immersed.

The f_2 similarity value between the two dissolution profiles reported in Figure 40 was 49, indicating that the two release profiles were different.

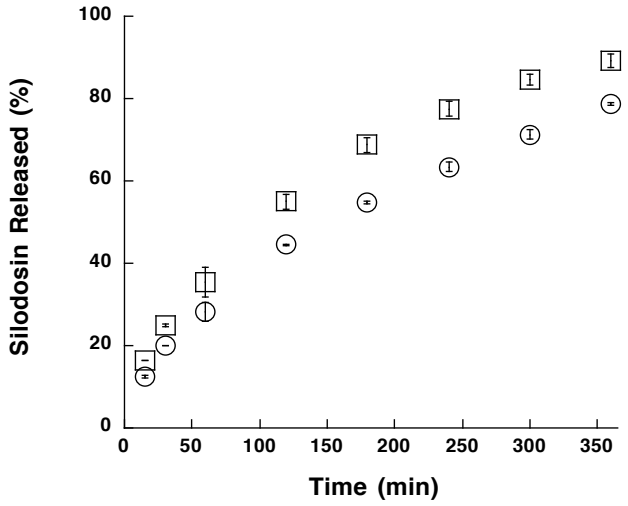

Figure 40. Release profiles of silodosin at pH 1.2 from the assembled system in void configuration: (○) without sinker and (□) in sinker (mean values ± standard deviations, n = 3).

As can be appreciated from the graph, the dissolution rate was higher when the assembled system was put in sinker, because of the greater surface area exposed to the medium. Nevertheless, from the kinetics analysis using the Ritger and Peppas equation [68,69], it was observed that the release mechanism (anomalous fickian) of the drug was similar in both cases (n = 0.57 ± 0.03 with sinker and n = 0.58 ± 0.02 without sinker). Then, the presence of sinker did not interfere with the swelling process.

At pH 3.5, the release of silodosin from the floating system after 4 hours was about 47%, while the drug release from the assembled system placed in the sinker was about 56% (Figure 41). In this case, the f_2 similarity value was 59, then the two release profiles were similar, even if the dissolution rate after 2 hours was slightly higher with sinker.

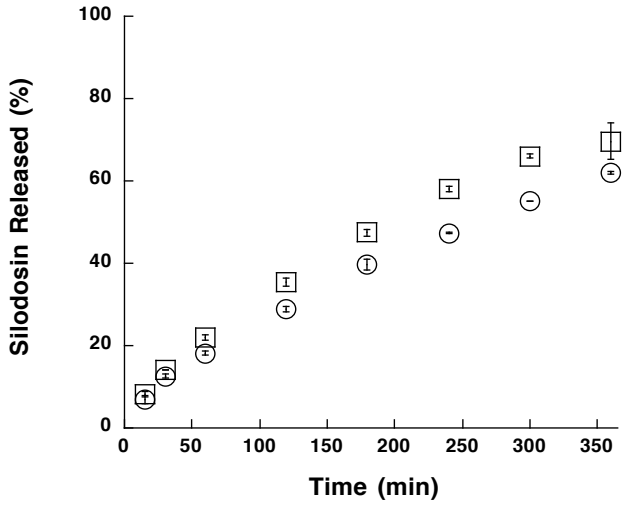

Figure 41. Release profiles of silodosin at pH 3.5 from the assembled system in void configuration: (○) without sinker and (□) in sinker (mean values ± standard deviations, n = 3).

However, the profiles tend more to the linearity (n = 0.61 ± 0.03 with sinker and n = 0.68 ± 0.03 without sinker), due to the reduced solubility of silodosin at pH 3.5.

4.3.7. Assembled system in void configuration containing 4 mg of silodosin

In order to have greater flexibility of dosing that best suit to the patient's needs, the 4 mg assembled system of silodosin, composed of two modules containing 2 mg each, was investigated.

A male module and a female module of silodosin 2 mg were assembled in void configuration. The *in vitro* dissolution tests at pH 1.2 and pH 3.5 of the assembled systems were carried out, both in sinker and without sinker. Without sinker, all the assembled systems floated immediately when immersed in the dissolution medium and the floatation lasted throughout the dissolution time.

The assembled systems placed in sinkers, when immersed in the dissolution medium, settled on the bottom of the vessel.

The release of silodosin from the floating system at pH 1.2 after 4 hours was about 65%, while in presence of sinker was about 74% (Figure 42), even if the two profiles were similar (f_2 = 60). From the kinetics analysis, n values (0.44 ± 0.01 with sinker and n = 0.40 ± 0.01 without sinker) showed that the release mechanism in both cases could be more diffusive.

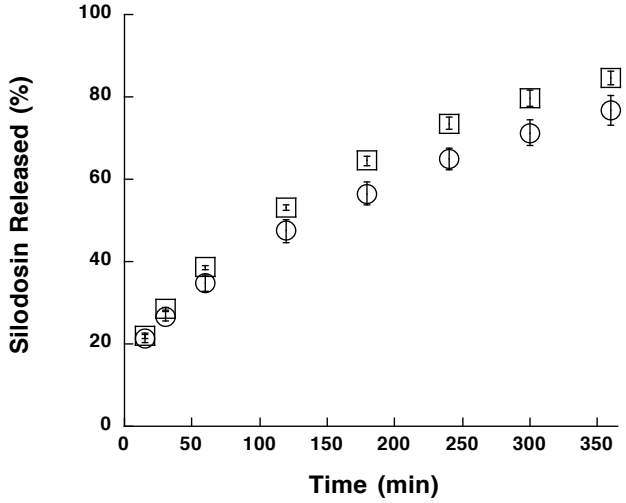

Figure 42. Release profiles of silodosin at pH 1.2 from the assembled system in void configuration: (○) without sinker and (□) in sinker (mean values ± standard deviations, n = 3).

At pH 3.5, the percentage of silodosin released after 4 hours was comparable with what observed at pH 1.2. Moreover, as noticed with the 4 mg + 4 mg assembled system, the reduced drug solubility at this pH led to a greater linearity of the release profiles.

Considering that an assembled system of 4 mg silodosin can be also obtained by interlocking a 4 mg module (female or male) with a placebo module (see section 4.3.4), in order to investigated if the partition of the drug amount in one module or two modules could affect the drug release and its mechanism, the release profiles obtained at pH 1.2 without sinker were compared (Figure 43).

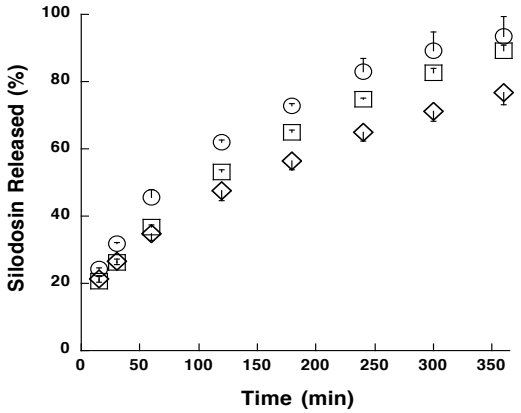

Figure 43. Release profiles of silodosin at pH 1.2 from the assembled system in void configuration: (○) silodosin 4 mg female module/placebo male module, (□) silodosin 4 mg male module/placebo female module and (◇) silodosin 2mg female module/silodosin 2mg male module (mean values ± standard deviations, n = 3).

As previously described in section 4.3.4, the release of silodosin from the 4 mg female module was higher than the male module when assembled with the placebo. On the other hand, when the amount of drug is distributed in the two modules the silodosin dissolution rate was reduced. This behaviour was supposed to be caused by the different drug/polymer ratio in the 2mg modules with respect to those containing 4mg. Besides, the kinetics analysis of the release profiles (0.44 ± 0.03 for 4 mg female module/placebo module assembled system, 0.46 ± 0.03 for 4 mg male module/placebo module assembled system and n = 0.40 ± 0.01 for 2 mg female module/2 mg male

module assembled system) exhibited a release mechanism mainly diffusive especially for the 2mg + 2mg silodosin assembled system.

4.3.8. Assembled system in void configuration containing 6 mg of silodosin

Still with a view to greater flexibility in the doses to be administered to the patients, the *in vitro* dissolution behavior of an assembled system containing 6 mg of silodosin was investigated. On the basis of the individual modules manufactured, four different combination of assembled modules were obtained, as summarized below:

A1. assembled system in mixed configuration made of three release modules containing each 2 mg of silodosin (terminal female module-stackable male module-terminal female module (FMF));

A2. assembled system in mixed configuration made of three release modules containing each 2 mg of silodosin (terminal female module-stackable female module-terminal male module (FFM)).

A3. assembled system in void configuration of a female module of silodosin 4 mg and a male module of silodosin 2 mg (FM);

A4. assembled system in void configuration silodosin of a male module of 4 mg and a female module of silodosin 2 mg (MF);

All assembled systems were analyzed in terms of *in vitro* dissolution at pH 1.2 and 3.5, with sinker and without sinker.

Assembled systems A1 and A2

During the dissolution test without sinker, both at pH 1.2 and pH 3.5, all the assembled systems, started to float after 2 minutes from their immersion in the medium and the floatation lasted throughout the dissolution time. At pH 1.2 the assembled systems FMF and FFM did not show a significant difference in the amount of drug released when the systems floated and the release profiles were superimposable (Figure 44A). The release mechanism analysis denoted that the anomalous fickian was predominant (n = 0.58 ± 0.06 for FMF (A1) configuration and n = 0.56 ± 0.01 for FFM (A2) configuration). Then, the different position of the female and male modules in the assembled systems seems to have no effect on the kinetics of drug released. When the assembled systems were placed in the sinker the drug profiles from FMF (A1) or FFM (A2) were not significant different (f_2 > 50 in both cases), even if the percentage of silodosin released from FMF (A1) was slightly higher than from FFM (A2) after 3 hours (Figure 44B).

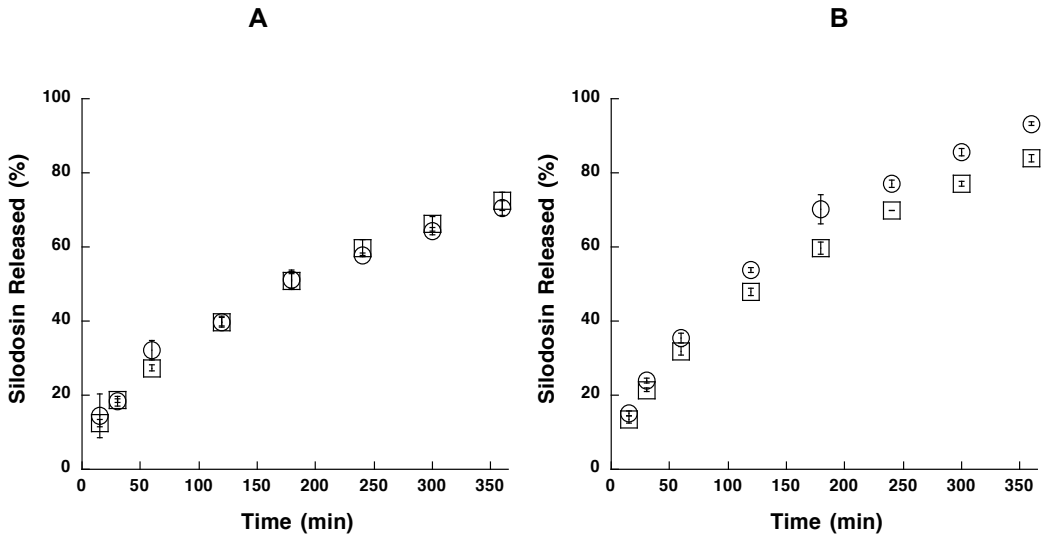

Figure 44. Release profiles of silodosin 6 mg at pH 1.2 from the assembled system in mixed configuration: (○) FMF and (□) FFM A) without sinker B) in sinker (mean values ± standard deviations, n = 3).

Even in the case of the *in vitro* dissolution at pH 3.5, not significant differences were observed between the two assembled systems A1 and A2 (Figure 45). Compared to what was observed at pH 1.2, as expected the drug released at pH 3.5 decreased due to the lower drug solubility at this pH and the release profiles tend to linearity.

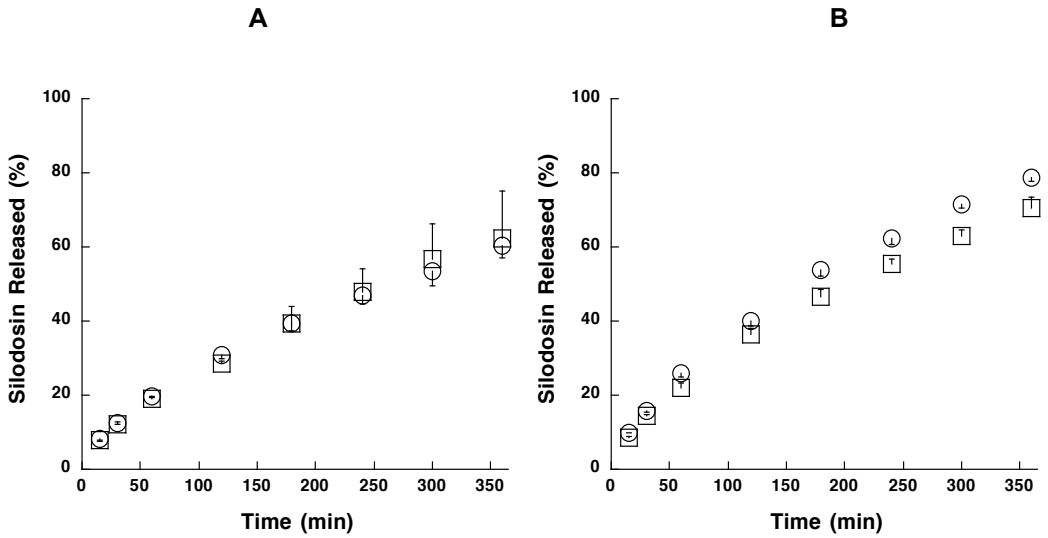

Figure 45. Release profiles of silodosin 6 mg at pH 3.5 from the assembled system in mixed configuration: (○) FMF and (□) FFM A) without sinker B) in sinker (mean values ± standard deviations, n = 3).

Assembled system A3 and A4

As already evidenced in the previous section, at pH 1.2 the assembled systems A3 (FM) and A4 (MF) did not show significant differences between them in the amount of drug released for both the dissolution test in sinker or without sinker (Figure 46). Even for the assembled systems A3 and A4 the release mechanism could be attributed to anomalous fickian (n = 0.68 ± 0.03 for FM (A3) configuration and n = 0.68 ± 0.07 for MF (A4) configuration).

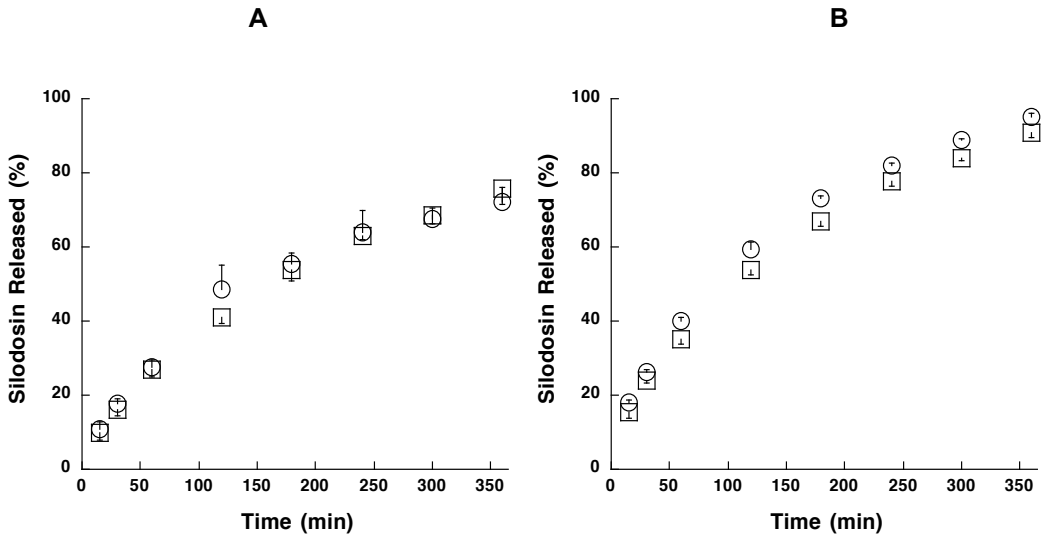

Figure 46. Release profiles of silodosin 6 mg at pH 1.2 from the assembled system in void configuration: (○) FM and (□) MF A) without sinker B) in sinker (mean values ± standard deviations, n = 3).

The release profiles of silodosin at pH 3.5 from A3 or A4 were practically superimposable, regardless of whether the dissolution tests were performed in sinker or without sinker.

The difference with respect to the dissolution at pH 1.2 is represented by the reduced percentage of drug released (Figure 47), due to the lower solubility of silodosin at pH 3.5.

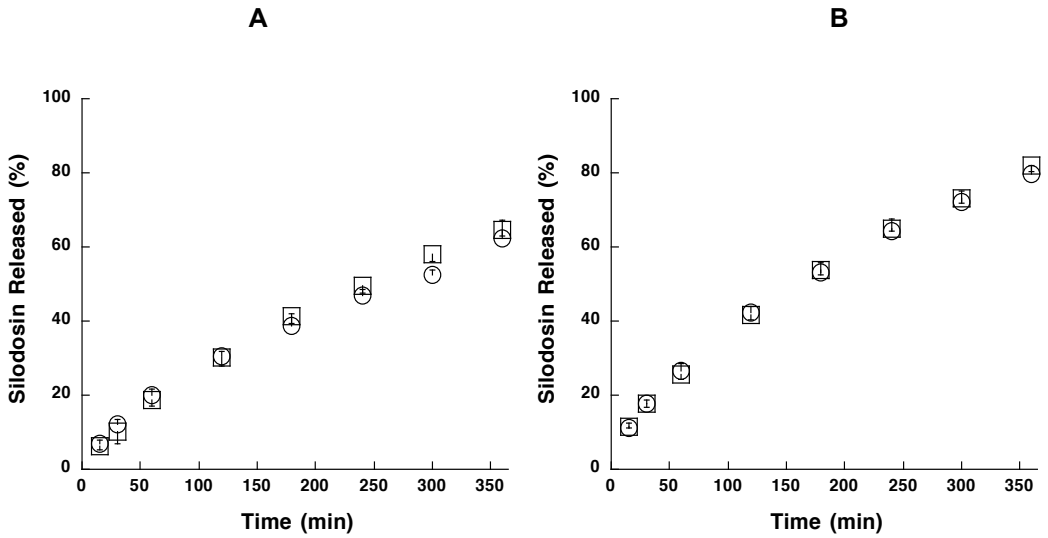

Figure 47. Release profiles of silodosin 6 mg at pH 3.5 from the assembled system in void configuration: (○) FM and (□) MF A) without sinker B) in sinker (mean values ± standard deviations, n = 3).

In summary, the study of the drug profiles obtained from the four different configurations (A1-A4) evidenced no difference between them (Figura 48), regardless of the amount of drug in the module and how the modules of different shape are positioned in the assembled system.

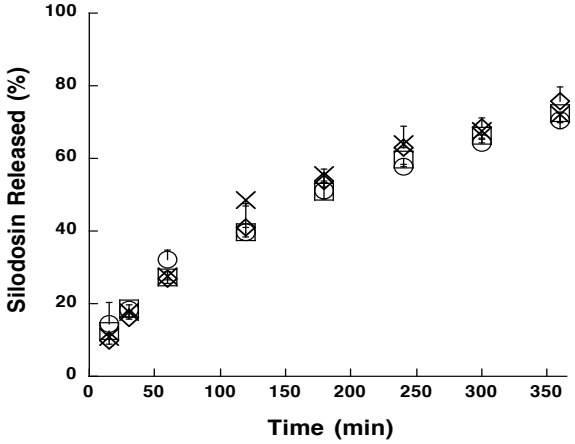

Figure 48. Release profiles of silodosin 6 mg at pH 1.2 from the assembled system: (○) FMF, (□) FFM, (×) FM and (◇) MF A) without sinker B) in sinker (mean values ± standard deviations, n = 3).

4.4. Characterisation of sildenafil citrate raw material

The active substance sildenafil citrate was characterised in terms of particle size distribution and solid state analyses.

The particle size measurement of the powder was carried out by laser light scattering Spraytec. The dimensional analysis of sildenafil citrate (Figure 49) showed a monodimensional distribution with Dv_{50} equal to 16.67 ± 0.96.

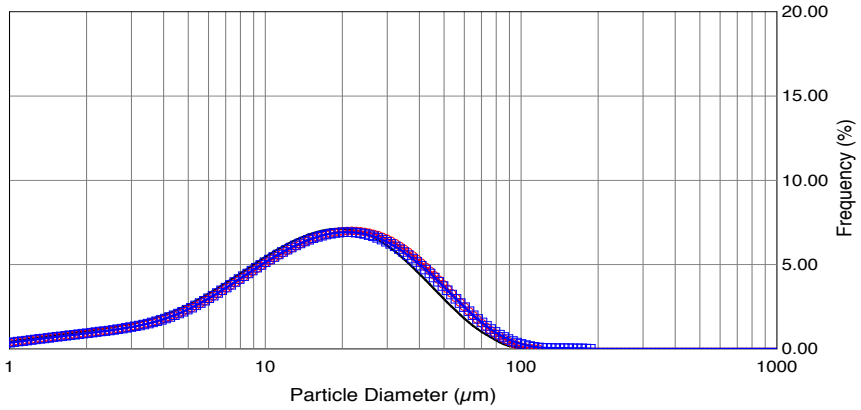

Figure 49. Dimensional distribution of sildenafil citrate powder.

The X-ray analysis of sildenafil citrate powder evidenced the presence of diffraction peaks, typical of drug crystalline structure (Figure 50).

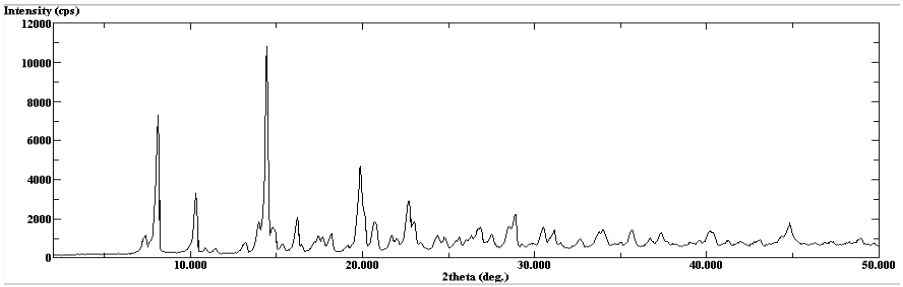

Figure 50. X-ray spectra of sildenafil citrate powder.

The DSC thermogram (Figure 51) showed the presence of an endothermic peak at 200 °C, corresponding to melting point of silodosin, in accordance with

the analysis certificate.

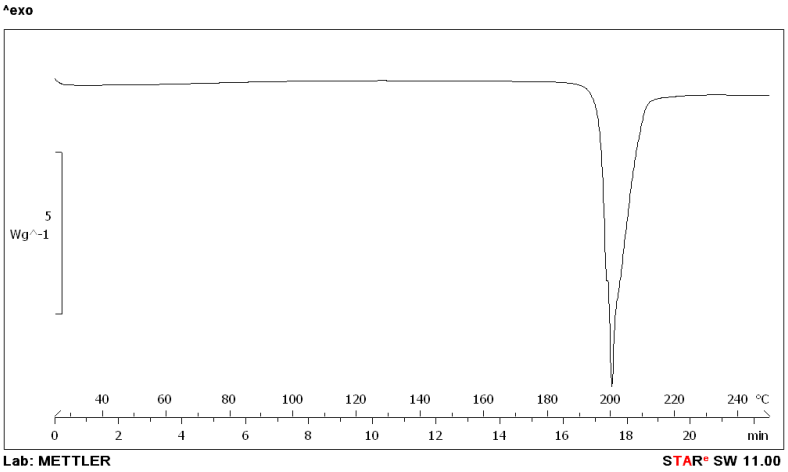

Figure 51. DSC curve of sildenafil citrate powder.

Table X shows the solubility values of sildenafil citrate at pH 1.2 and pH 3.5 at 37 ± 0.5 ° C. As can be observed from the values, the solubility of sildenafil citrate decrease as the pH increases.

Table X. Solubility of sildenafil citrate at 37 °C ± 0.5 ° C

Solubility	mg/mL
pH 1.2	42,60 ± 0,10
pH 3.5	7,20 ± 0,52

4.5. Validation of the HPLC method for the determination of sildenafil citrate

The HPLC method for the analysis of sildenafil citrate was validated according to the Ph. Eur. 8th Ed., considering the following parameters:

- Linearity: the linear relationship between the chromatogram signals and the analyte concentration by applying linear regression equation (Figure 52). The linear regression coefficient r^2 for sildenafil citrate was 0.99999.

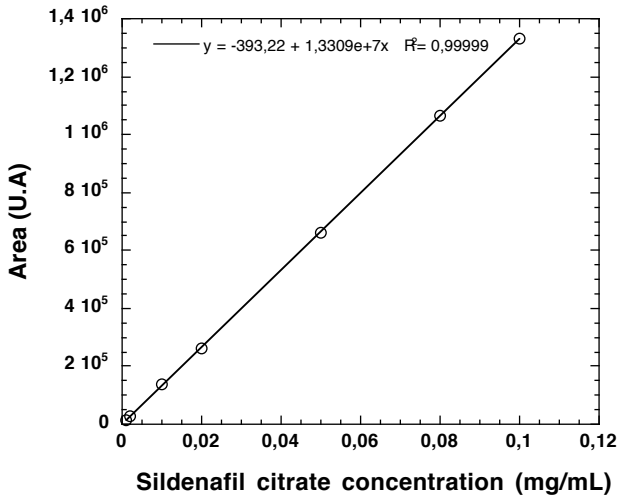

Figure 52. Area of chromatographic peaks obtained from sildenafil citrate solutions plotted vs their concentration.

- Theoretical plates: calculated using the following formula

$$N = \frac{t}{W^2}$$

where t indicates the retention time and W the width of the base of the peak. The number of theoretical plates (N) for sildenafil citrate was 3258.15 ± 115.10.

- Tailing factor: calculated using the following formula

$$T = \frac{W_{0.05}}{2f}$$

where $W_{0.05}$ indicates the peak width at 1/20 of its height, while f represents the distance between the perpendicular drawn from the peak maximum and the start point of the peak at 1/20 of its height. The tailing factor for the sildenafil citrate was 2.

4.6. Manufacturing of sildenafil citrate controlled release module

Female or male modules of sildenafil, containing 40 mg each of sildenafil citrate, were manufactured to be assembled with a module of silodosin in order to obtain a fixed dose combination product. Initially, the manufacturing of the modules (female and male) was carried out by direct compression of powder blend, the composition of which is reported in Table XI.

Table XI. Composition of sildenafil citrate 40 mg F#1 module.

Components	Weight (mg)	Percentage (w/w)
Sildenafil Citrate	40.0	33.4
Avicel PH102	20.0	16.7
Methocel K15M	35.0	29.4
Pearlitol 200 SD	20.0	16.7
Talc	3.45	2.9
Magnesium stearate	1.15	1.0
Total	**119.6**	**100**

During the compression of the powder, the female modules were easily obtained, while it was not possible to manufacture the male modules due to the fracture of the annular protrusion. In order to improve the cohesion property of the powder and the compression process of the male modules, as in the case of silodosin, a wet granulation of sildenafil was carried out. By varying the composition of excipients and their amount, different granulate formulations of sildenafil citrate were prepared (Table XII). At each formulation 3% of talc and 1% of magnesium stearate were added extra-granular and compressed to obtain both female and male modules.

Table XII. Composition of granulates of sildenafil citrate 40 mg (amount for 100 modules).

Components	F#2	F#3	F#4	F#5	
Sildenafil Citrate	0.4	0.4	0.4	0.4	g
Avicel PH102	2.39	2.39	2.69	1.8	g
Methocel K15M	2.20	-	1.6	1.5	g
Methocel K4M	-	2.20	-	-	g
Pearlitol 200 SD	2.39	2.39	2.69	1.8	g
Beta-cyclodextrin	-	-	-	4.0	g
Water	4	3.5	3.5	3.5	mL

As already done in the case of silodosin, before carrying out *in vitro* dissolution tests, the stability of sildenafil was investigated in the two media (pH 1.2 and pH 3.5). The HPLC analysis did not show the presence of other chromatographic peaks apart that corresponding to sildenafil citrate. Moreover, no significant

decrease in the drug amount (%) was observed (Figure 53).

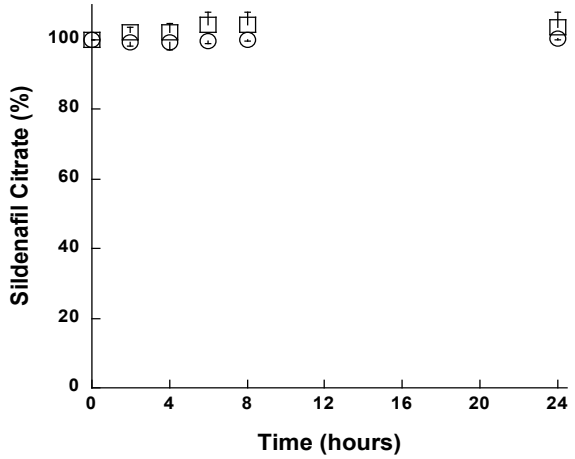

Figure 53. Stability of sildenafil citrate at pH 1.2 (○) and pH 3.5 (□) (mean ± standard deviation, n = 3).

To identify the granulate formulation more promising in terms of drug release from an assembled system of 60% after 4 hours of dissolution, a female module containing sildenafil citrate was assembled with a male placebo module in void configuration. The dissolution profiles at pH 1.2 are showed in Figure 54.

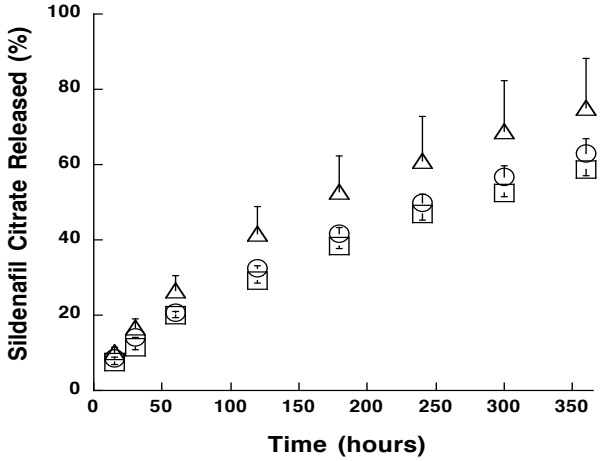

Figure 54. Release profiles of the assembled system in void configuration of sildenafil citrate 40 mg female module/placebo male module (○) F#2, (□) F#3, (△) F#4 at pH 1.2 (mean values ± standard deviation, n = 3).

The female module of sildenafil citrate, obtained with formulation F#2, showed a drug release of approximately 50% after 240 minutes. Since the drug release target from both drugs (silodosin and sildenafil citrate) in the assembled system was 60% in the first four hours, the granulate formulation was modified.

In the case of F#3, the polymer Methocel K15M (viscosity 15,000 mPa s) was replaced with one having a lower viscosity (Methocel K4M, viscosity 4,000 mPa s). The change of HPMC type did not led to an improvement of the dissolution profile of the sildenafil citrate from the female module.

Then, in the formulation F#4 was used again HPMC K15M, but the percentage was reduced from 22% to 16%. After 4 hours of dissolution at pH 1.2, an increase in the percentage of drug released (about 60% after 240 minutes) was observed.

It was added beta-cyclodextrine to the formulation with the objective to increasing the solubility of the drug (F#5). The dissolution profile of the sildenafil citrate female module obtained with the formulation F#5 was almost comparable with that showed in case of formulation F#4 (Figure 55). The addition of b- cyclodextrin to the formulation did not result in an increase of drug released after 4 hours, but it reduced the variability in terms of standard deviation. For this reason, the formulation F#5 was used for the manufacture of the sildenafil citrate modules. Table XIII shows the module composition.

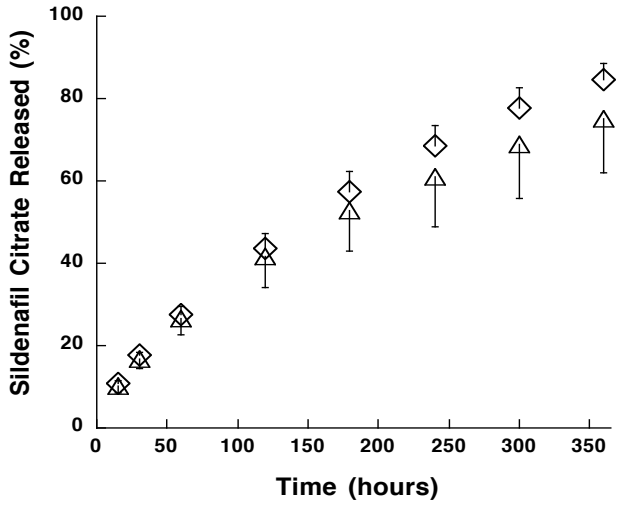

Figure 55. Release profiles of the assembled system in void configuration of sildenafil citrate 40 mg female module/placebo male module (△) F#4 and (◇) F#5 at pH 1.2 (mean values ± standard deviations, n = 3).

Table XIII. Composition of sildenafil citrate 40 mg F#6 module.

Components	Weight (mg)	Percentage (w/w)
Sildenafil Citrate	40.0	29.4
Avicel PH102	18.0	13.2
Methocel K15M	15.0	11.0
Pearlitol 200 SD	18.0	13.2
Beta-cyclodextrin	40.0	29.4
Talc	3.93	2.9
Magnesium stearate	1.31	1.0
Total	**136.24**	**100**

The granulate of sildenafil F#6 was then characterized.

The analysis of the size distribution, performed with the sieve test, is showed in Figure 56. As can be observed from the graph, the dimensions of the granules were mainly distributed between 250 and 500 μm.

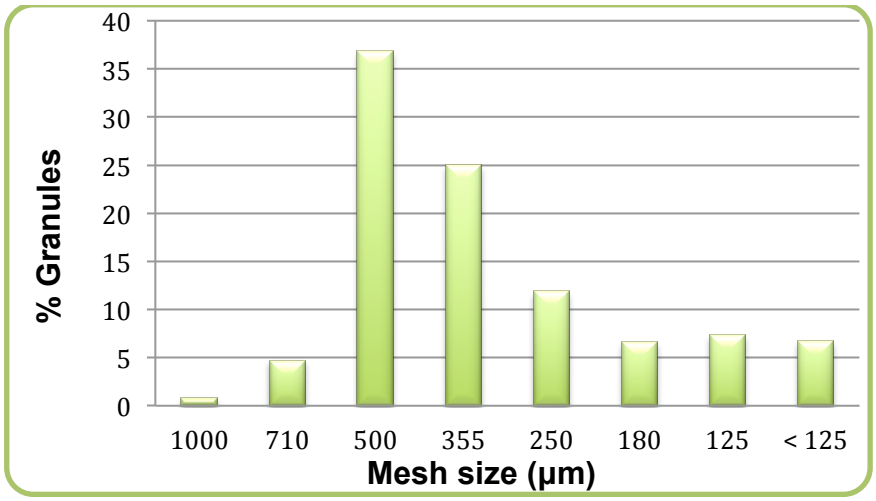

Figure 56. Dimensional distribution of sildenafil citrate 40 mg F#6 granules.

The granulate of sildenafil citrate was also characterised in terms of residual moisture content, tapped density and bulk density.

The residual moisture content, determined with a volumetric titration, showed a value of 2.29 ± 0.24% (w/w). The results of bulk density test showed a value of 0.31 g/mL, while the tapped density was 0.41 g/mL.

The sildenafil citrate modules were characterised in terms of weight, height and diameter (Table XIV).

Table XIV. Values of weight, height and diameter of male and female terminal modules of sildenafil 40 mg F#6 (mean ± standard deviation).

	Weight (mg)	Height (mm)	Diameter (mm)
Terminal Female	136.1 ± 3.73	4.54 ± 0.07	7.57 ± 0.01
Terminal Male	138.2 ± 4.10	4.65 ± 1.87	7.55 ± 0.01

The male and female modules showed a friability value of 0.15% and 0.22% respectively, according to the specifications of Ph. Eur. 8th Ed. The values of the

hardness of the modules, in both diametral and axial orientations, are summarized in Table XV.

Table XV. Hardness of male and female terminal modules of sildenafil 40 mg F#6.

	Diametral (N)	Axial (N)
Terminal Female	51.01 ± 4.41	72.59 ± 4.41
Terminal Male	78.48 ± 6.97	102.02 ± 8.73

The dissolution profiles of the male and female modules of sildenafil citrate at pH 1.2 are illustrated in Figure 57. During the *in vitro* dissolution test the individual modules were placed into the sinker. The release of the sildenafil citrate from the female and the male modules after 4 hours was about 100% and 90%, respectively.

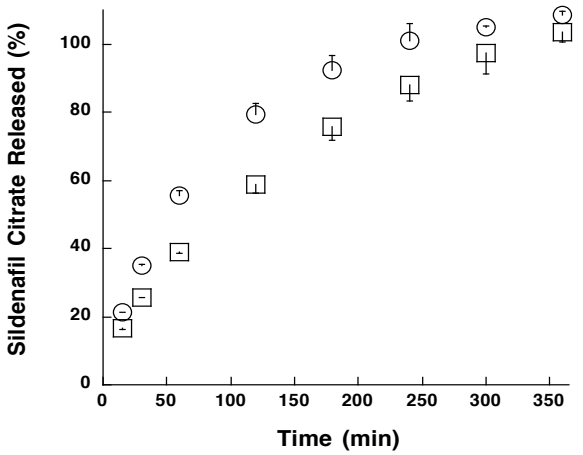

Figure 57. Release profile of sildenafil citrate 40 mg F#6 at pH 1.2 with sinker (O) female module and (□) male module (mean ± standard deviation, n = 3).

The dissolution profiles of the male and female modules of sildenafil citrate at

pH 3.5 in sinker are illustrated in Figure 58.

The release of the sildenafil citrate from the female and male modules after 4 hours was about 75% and 60%, respectively. The reduced solubility of sildenafil citrate at pH 3.5 (see Table X) led to a lower % of drug released at this pH; moreover, as expected, the release profiles were more linear.

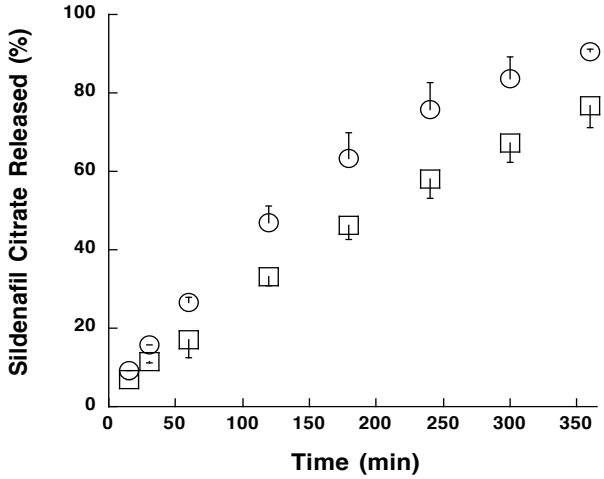

Figure 58. Release profile of sildenafil citrate 40 mg at pH 3.5 in sinker (O) female module and (□) male module (mean ± standard deviation, n = 3).

4.6.1. Assembled system of sildenafil citrate 40 mg module with placebo module

In order to exclude any possible interference between the two modules containing each an active ingredient (silodosin or sildenafil citrate) when they were assembled in void configuration, the study of *in vitro* release of sildenafil citrate with placebo module was carried out, as previously done for silodosin modules. Both sildenafil citrate female and male modules were assembled in void configuration with a placebo male module and a placebo female module, respectively. The composition of the placebo module is the one reported in

Table IX. The release profiles of the assembled systems at pH 1.2 and pH 3.5 are reported in Figure 59. Both the assembled systems floated immediately when immersed in the dissolution medium and the floatation lasted throughout the dissolution time. No disintegration was observed. The release of sildenafil citrate at pH 1.2 after 4 hours from the female module combined with the placebo male module was about 63% while the release from the individual female module was about 100% (see Figure 57). The release from the male module combined with a placebo female module was about 44% while the release from the individual male module was about 90%. The release of sildenafil citrate at pH 3.5 after 4 hours from the female module combined with the placebo male module was about 26% while the release from the individual female module was about 75% (see Figure 58). The release from the male module combined with a placebo female module was about 20% while the release from the individual male module was about 60%.

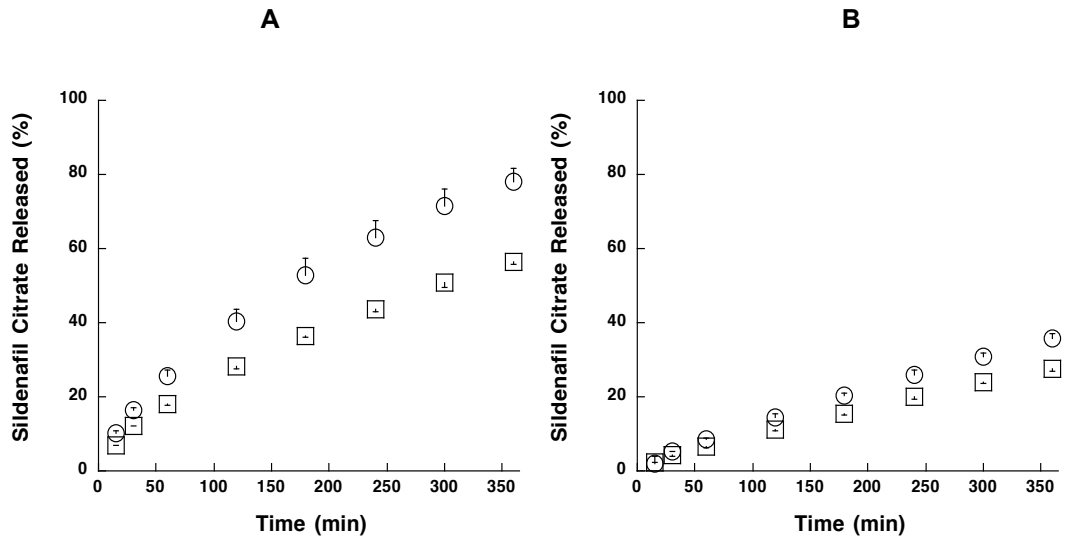

Figure 59. Release profiles of the assembled system in void configuration of (○) sildenafil citrate mg female module/placebo male module (□) and sildenafil citrate male module/placebo female module A) pH 1.2 and B) pH 3.5 (mean ± standard deviation, n = 3).

4.6.2. Assembled system of sildenafil citrate 40 mg module and silodosin 4 mg module

An assembled system in void configuration, consisting of silodosin 4 mg and sildenafil citrate 40 mg, was investigated in order to obtain a floating system. The system was obtained assembling the modules in two different combinations in void configuration. The first one was composed by a female module of sildenafil citrate and a male module of silodosin. The second combination was composed by a female module of silodosin and a male module of sildenafil citrate.

The *in vitro* dissolution test of the assembled systems was performed at pH 1.2 and pH 3.5 with and without sinker. All the assembled systems floated immediately when immersed in the dissolution medium and the floatation lasted throughout the dissolution time. No disintegration was observed.

The release profiles of the two drugs (Figure 60A, without sinker) shows that the assembled system made of sildenafil citrate female module and silodosin male module released after 4 hours 66% of sildenafil and 63% of silosodin. In contrast, inverting the drug module combination (sildenafil citrate male module and silodosin female module), the release of sildenafil citrate was 52% while while the release of silodosin was 71% (Figure 60B, without sinker).

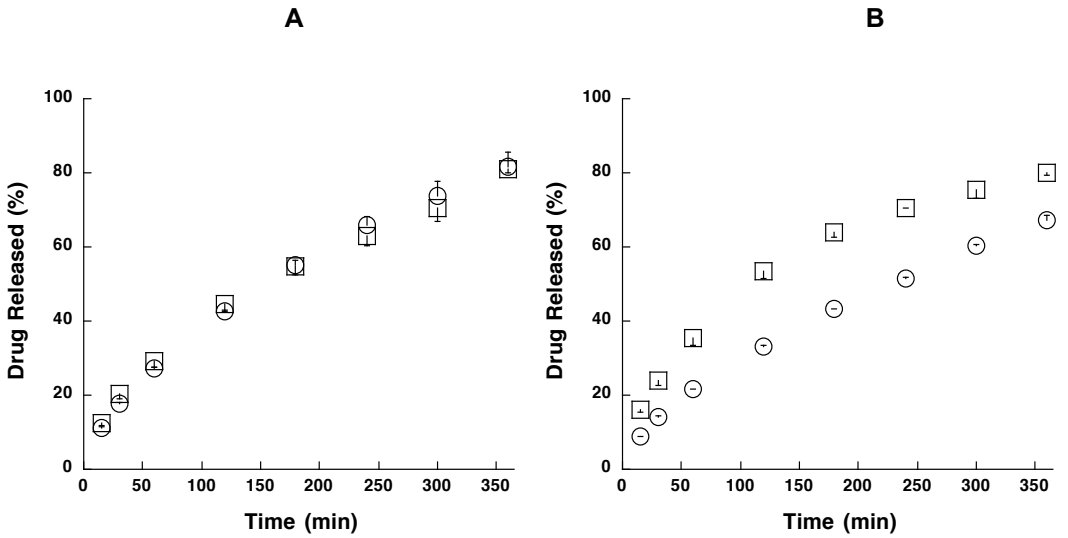

Figure 60. Release profiles of the assembled system in void configuration at pH 1.2 of A) (○) sildenafil citrate female module and (□) silodosin male module B) (○) sildenafil citrate male module and (□) silodosin female module (mean ± standard deviation, n = 3).

It is interesting to evidence how the release profiles of the two drugs depend in which module the drug is contained. In the case of assembled system made of the female module containing sildenafil and the male module containing silodosin, the release profiles of the two drugs are superimposable. Instead, in the case of the assembled system composed by the male module containing sildenafil and female module containing silodosin the two release profiles are different. In fact, the release from the male module of sildenafil is slower compared to the release of the female module containing silodosin.

The same behavior was observed in the dissolution test carried out with sinker. Figure 61A shows that the release of silodosin from the male module was 68% and the release of sildenafil citrate from the female module was 70% after 4 hours of dissolution. Instead, inverting the drug module composition, the release of silodosin was 77% while the release of sildenafil citrate was 58% as shown in the Figure 61B.

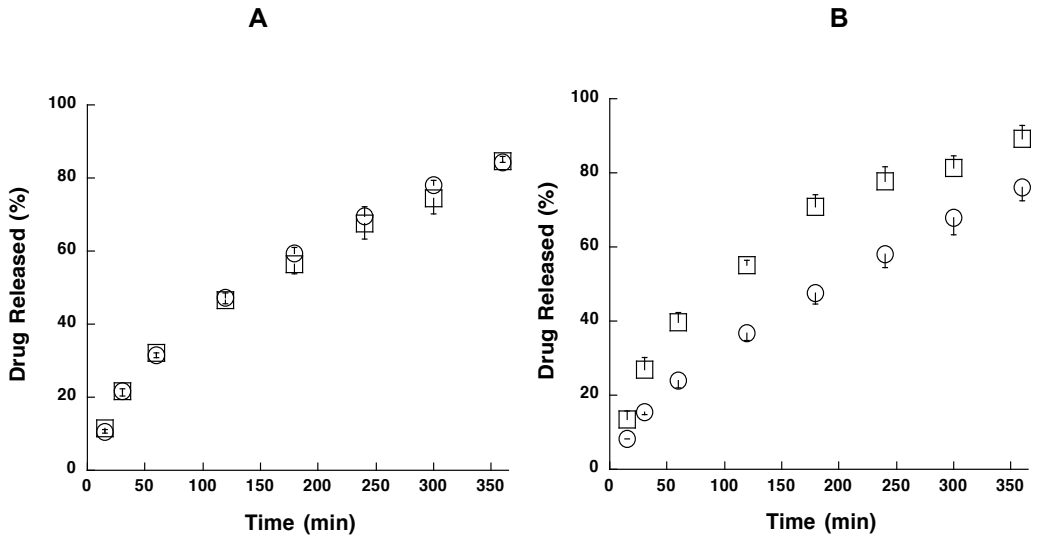

Figure 61. Release profiles of the assembled system in void configuration at pH 1.2 in sinker of A) (○) sildenafil citrate female module and (□) silodosin male module B) (○) sildenafil citrate male module (□) and silodosin female module (□) (mean ± standard deviation, n = 3).

Figure 62 shows the release profiles of the two drugs at pH 3.5 without sinker. The assembled system composed by the female module containing sildenafil citrate and the male module containing silodosin released after 4 hours 28% of sildenafil and 55% of silosodin (Figure 62A). Instead, inverting the drug module composition, the release of silodosin was 62% while the release of sildenafil citrate was 22% as shown in the Figure 62B.

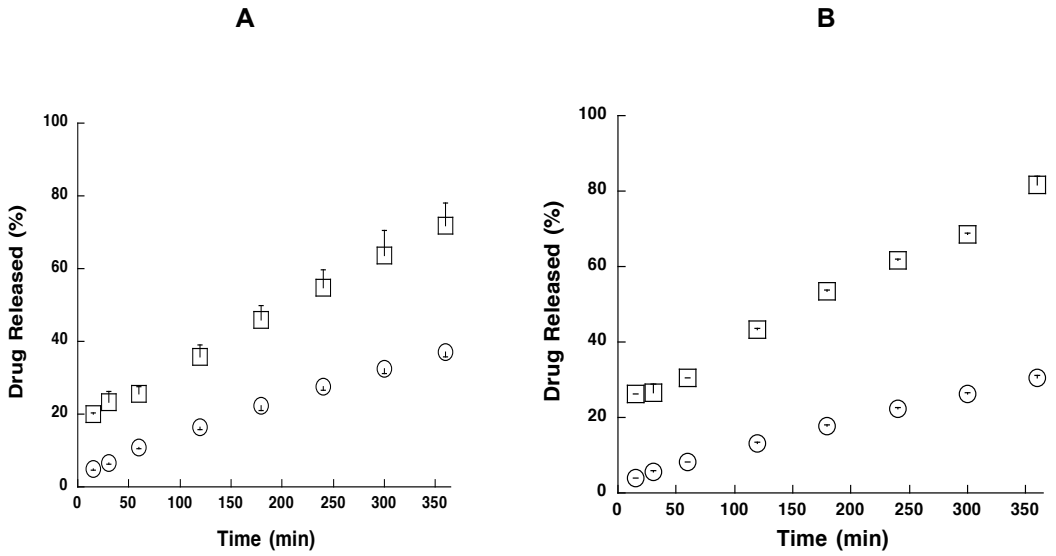

Figure 62. Release profiles of the assembled system in void configuration at pH 3.5 of A) (○) sildenafil citrate female module and (□) silodosin male module B) (○) sildenafil citrate male module and (□) silodosin female module (mean ± standard deviation, n = 3).

Figure 63 shows the release profiles of the two drugs at pH 3.5 in sinker.

The assembled system composed by the female module containing sildenafil citrate and the male module containing silodosin released after 4 hours 38% of sildenafil and 53% of silosodin (Figure 63A).

Instead, inverting the drug module composition, the release of silodosin was 65% while the release of sildenafil citrate was 30% as shown in the Figure 63B.

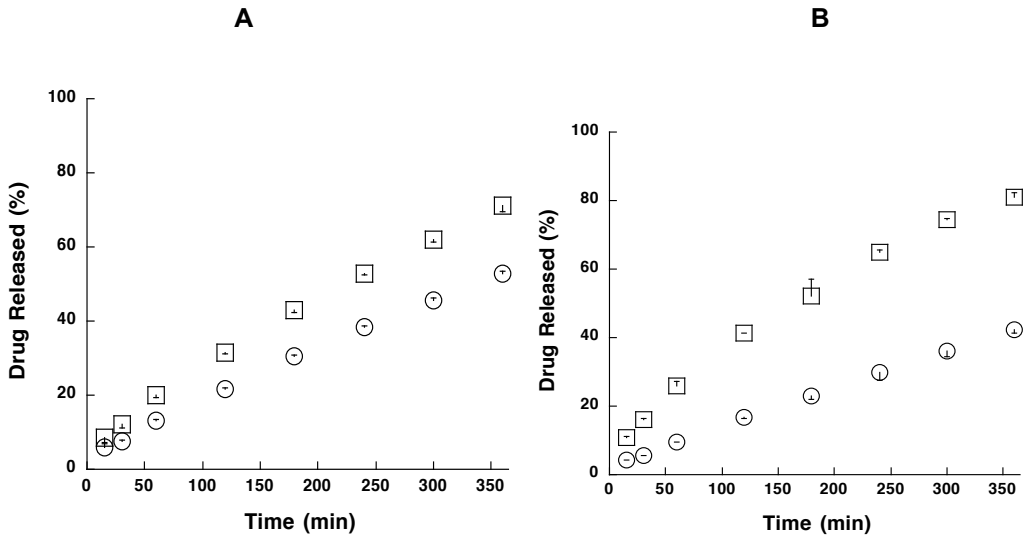

Figure 63. Release profiles of the assembled system in void configuration at pH 3.5 in sinker of A) (○) sildenafil citrate female module and (□) silodosin male module B) (○) sildenafil citrate male module and (□) silodosin female module (mean ± standard deviation, n = 3).

The dissolution profiles of the assembled systems of sildenafil citrate and silodosin at pH 1.2 and pH 3.5 showed different behavior. The possibility to have the same release profiles of the two drugs, (combination of sildenafil female module and silodosin male module) obtained at pH 1.2 did not occurred at pH 3.5. This because of the drastic decrease of the sildenafil citrate solubility at this pH value.

4.7. Swelling studies of the individual modules and the assembled systems

The study of swelling behavior was carried out by gravimetric procedure on silodosin 4 mg, silodosin 2 mg and sildenafil citrate 40 mg individual modules and their assembled systems previously described.

4.7.1. Swelling behaviour of silodosin 4 mg F#B modules

In Figure 64 the swelling profiles of individual silodosin modules (4 mg) and the 8 mg assembled systems in void configuration at pH 1.2 and pH 3.5 are shown.

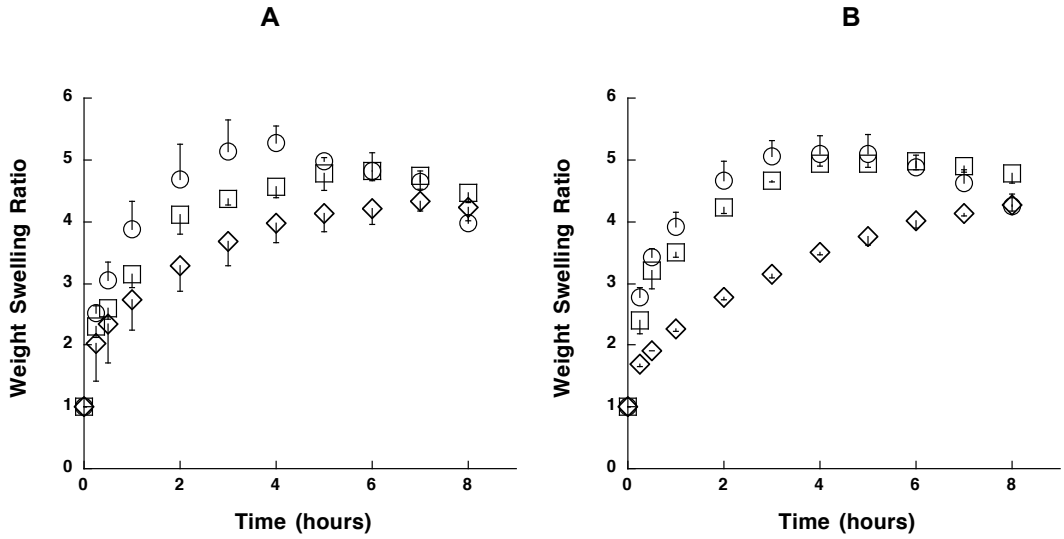

Figure 64. Swelling profiles of silodosin 4 mg, (○) female module, (□) male module and (◇) void configuration at A) pH 1.2 and B) pH 3.5 (mean ± standard deviation, n = 3).

The swelling ratio of the female module at pH 1.2 was higher than the male module and the erosion process occurred before. This is due to the shape of the female module that is more exposed to the dissolution medium. The swelling profile of the assembled system was lower than the individual modules because the surface exposed to the medium is smaller as the two concave

bases of the modules were not in direct contact with the medium. These results confirmed what observed in the dissolution behavior of the individual modules and the assembled systems.

At pH 3.5 the difference in terms of swelling ratio of the individual modules was less appreciable but anyway higher for the female module.

The presence of different media, as simulated gastric fluid with pepsin at pH 1.2 and simulated intestinal fluid at pH 6.8, did not affect the swelling ratio of the assembled system (Figure 65). No substantial differences between the two swelling profiles in the two different media were evidenced.

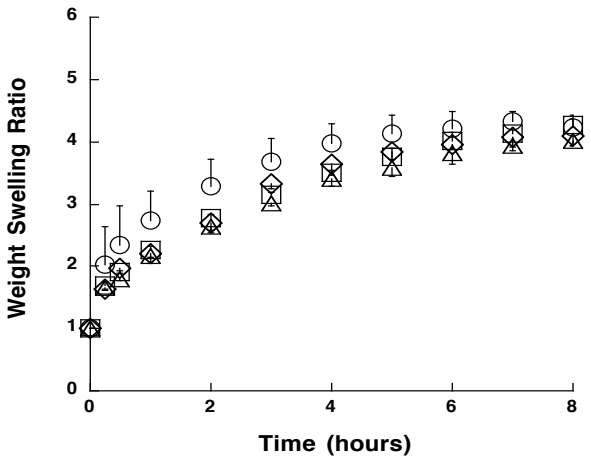

Figure 65. Swelling profiles of silodosin 8 mg assembled system in void configuration at (○) pH 1.2, (□) pH 3.5, (◇) pH 1.2 with pepsin and (△) pH 6.8 (mean ± standard deviation, n = 3).

4.7.2. Swelling behaviour of silodosin 2 mg F#A modules

In Figure 66 the swelling profiles of individual modules (2 mg) and the 4 mg assembled system in void configuration at pH 1.2 and pH 3.5 are reported.

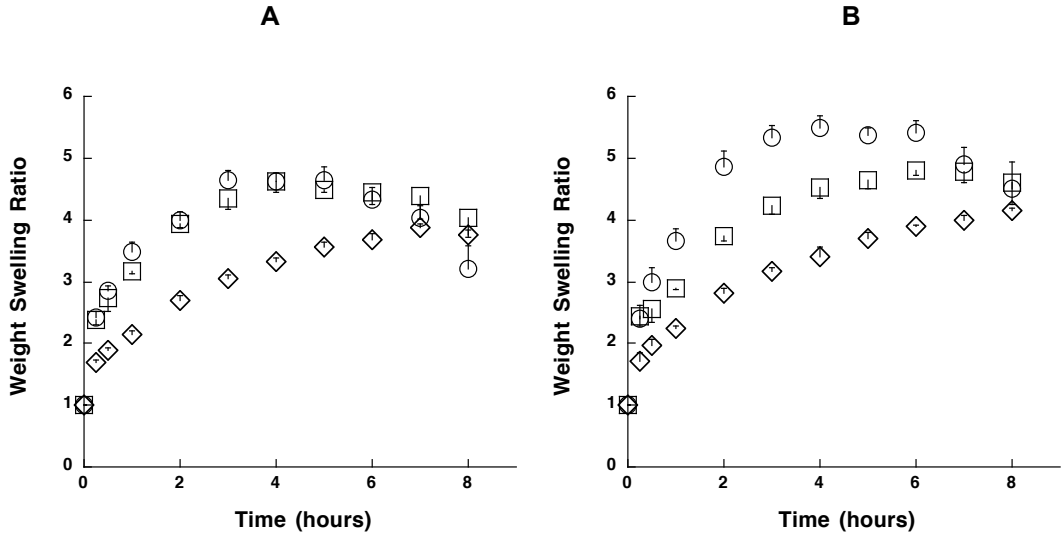

Figure 66. Swelling profiles of silodosin 2 mg, (○) female module, (□) male module and (◇) void configuration at A) pH 1.2 and B) pH 3.5 (mean ± standard deviation, n = 3).

In this case the swelling ratio of the individual female and male modules is clearly different at pH 3.5. The 2 mg female module showed an higher swelling ratio with respect of the 2 mg male module. This could be due to the fact that the higher surface area of the female module, exposed to the dissolution medium, contributed to the increase of swelling ratio despite the drug solubility at pH 3.5 is lower. This phenomenon was not observed in the modules containing 4 mg of silodosin (Figure 66B) and this could related to the different drug/polymer ratio in the types of modules (2 mg and 4 mg).

4.7.3. Swelling behaviour of silodosin assembled system (2 mg + 2 mg + 2 mg)

The swelling behaviour of the two combinations FFM and FMF was investigated. The experiments were carried out only in simulated gastric fluid without enzymes at pH 1.2. The swelling profiles are showed in Figure 67.

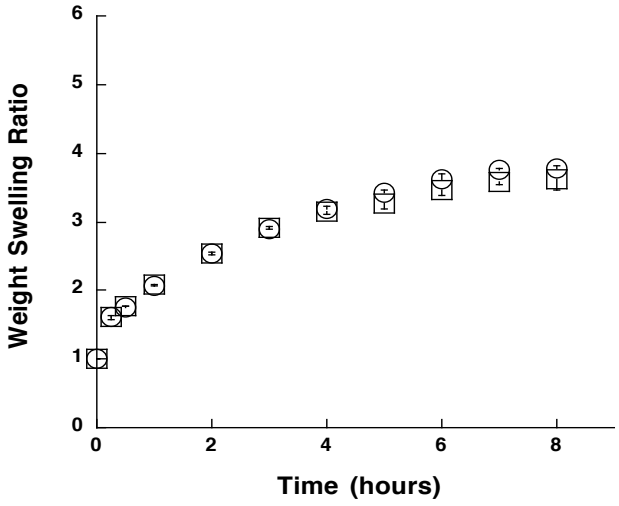

Figure 67. Swelling profiles of silodosin 2 mg + 2 mg + 2 mg in mixed configuration (○) FFM and (□) FMF at pH 1.2 (mean ± standard deviation, n = 3).

No significant differences of swelling behaviour between the two combinations were evidenced. These results confirmed those obtained from the in vitro dissolution test (Figure 44A).

4.7.4. Swelling behaviour of sildenafil citrate 40 mg modules

The swelling behaviour of the individual modules containing sildenafil citrate was investigated. The experiments were carried out in simulated gastric fluid without enzymes at pH 1.2 and fluid at pH 3.5. The swelling profiles are showed in Figure 68.

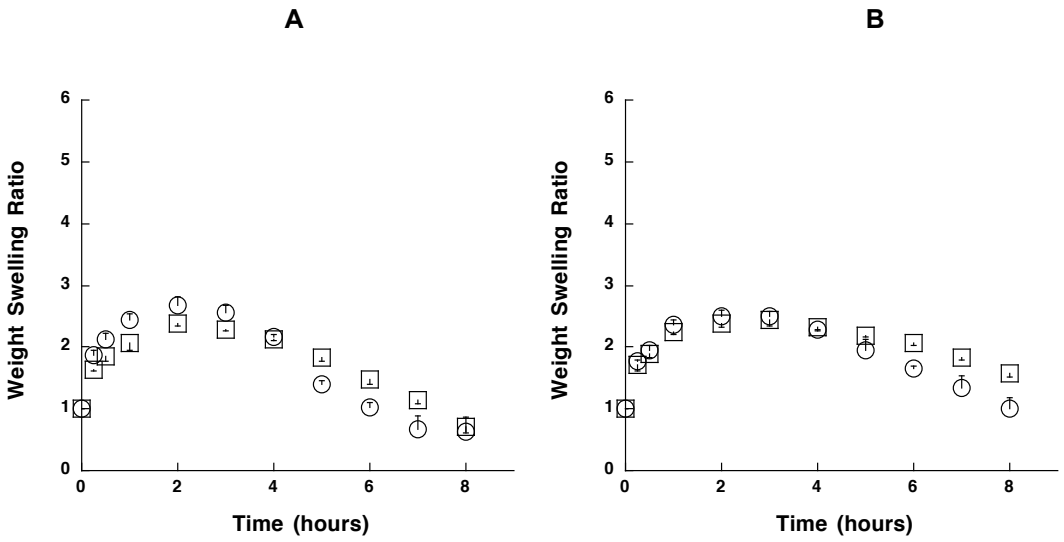

Figure 68. Swelling profiles of sildenafil citrate 40 mg female module (○) and male module (□) at A) pH 1.2 and B) pH 3.5 (mean ± standard deviation, n = 3).

The swelling ratio of the female module is higher than the male module and the erosion process occurred before. Moreover, the swelling ratio was higher at pH 1.2 than pH 3.5.

4.7.5. Swelling behaviour of silodosin 4 mg and sildenafil citrate 40 mg assembled system

The swelling behaviour of the assembled systems containing sildenafil citrate and silodosin was investigated. The experiments were carried out in simulated gastric fluid with and without enzymes at pH 1.2, fluid at pH 3.5 and simulated intestinal fluid at pH 6.8. The swelling profiles are showed in Figure 69.

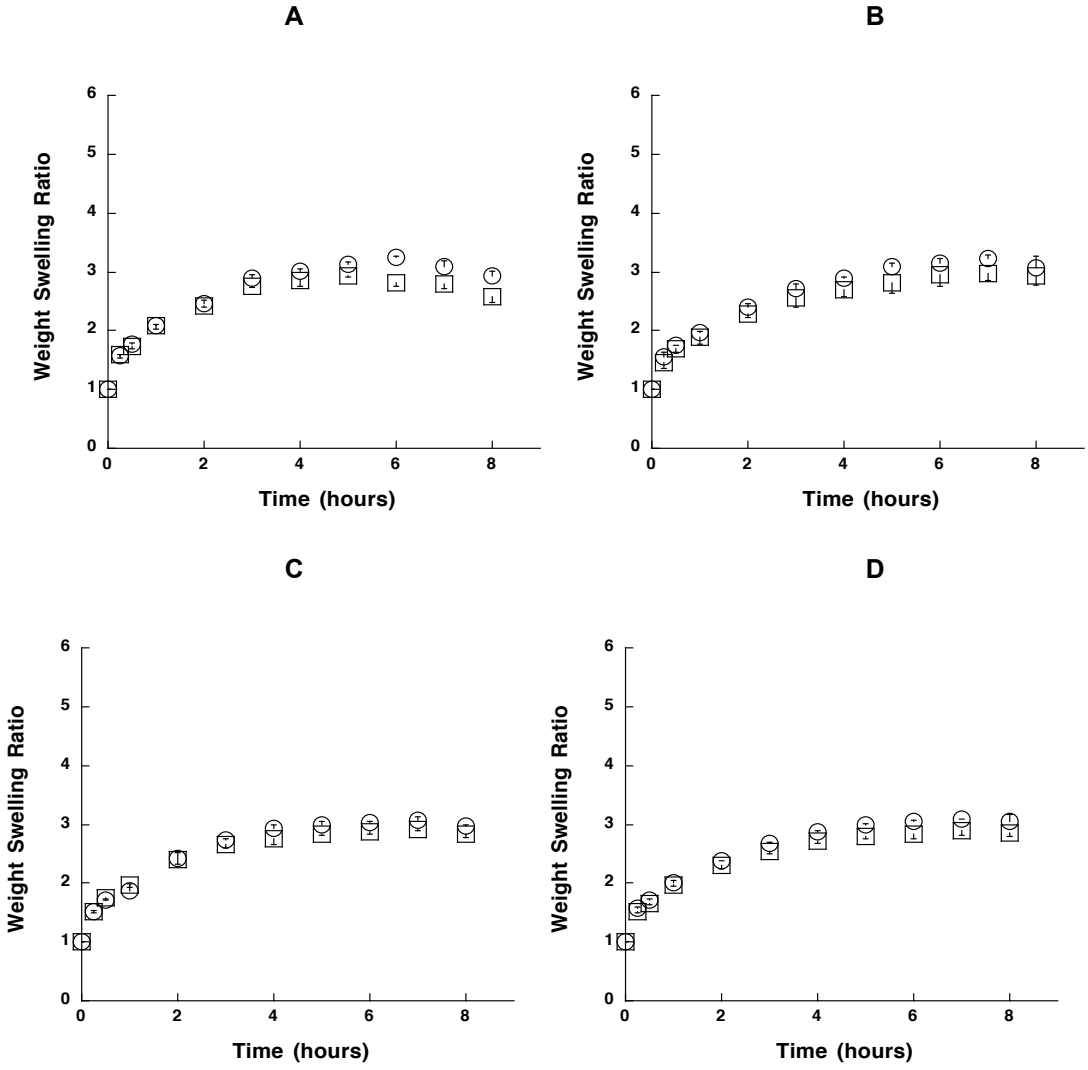

Figure 69. Swelling profiles of void configuration of (○) silodosin 4 mg female module/sildenafil citrate 40 mg male module and (□) silodosin 4 mg male module/sildenafil citrate 40 mg female at A) pH 1.2, B) pH 3.5, C) pH 1.2 with pepsin and D) pH 6.8 (mean ± standard deviation, n = 3).

The assembled systems of sildenafil citrate and silodosin in the two combinations did not show significant differences of swelling behaviour varying the media.

4.8. High Resolution X-ray Computed Tomography

The analysis of the polymer swelling and the phenomena connected to it (for example dissolution, erosion etc.) are important for the interpretation of the release kinetics of the swellable matrices. The literature reports some techniques to measure the movement of the fronts such as photographic technique, nuclear magnetic resonance imaging or microscope with polarized light. In the present work, the process of dissolution and swelling of Dome Matrix modules has been studied by High-Resolution X-ray Computed Tomography. The measuring principle of tomography is based on the different absorption of radiation of X-rays depending on the density of the sample. Basically, the data of relative density distribution of many sections of the sample are processed in order to reconstruct an electronic image of the sample in which identify the portions of material with different densities. This reconstruction technique in three dimensions is called "surface rendering". The experiments were carried out at the Department of Geological Sciences, University of Texas at Austin (Austin, USA). The experiments were performed by placing the assembled systems in simulated gastric fluid without enzymes at pH 1.2. Their behaviour was studied for 3 hours. The X-ray computed tomography images, collected at fixed time (15, 30, 45, 60, 120 and 180 min) permitted to observe the variations occurring in the assembled systems in

contact with the dissolution medium. Figure 70 illustrates the behaviour of the assembled system made of two modules of silodosin 2 mg in a void configuration at different times in pH 1.2. It can be observed as the separation of the particles increased with time and the density of the system changed in contact with the dissolution medium.

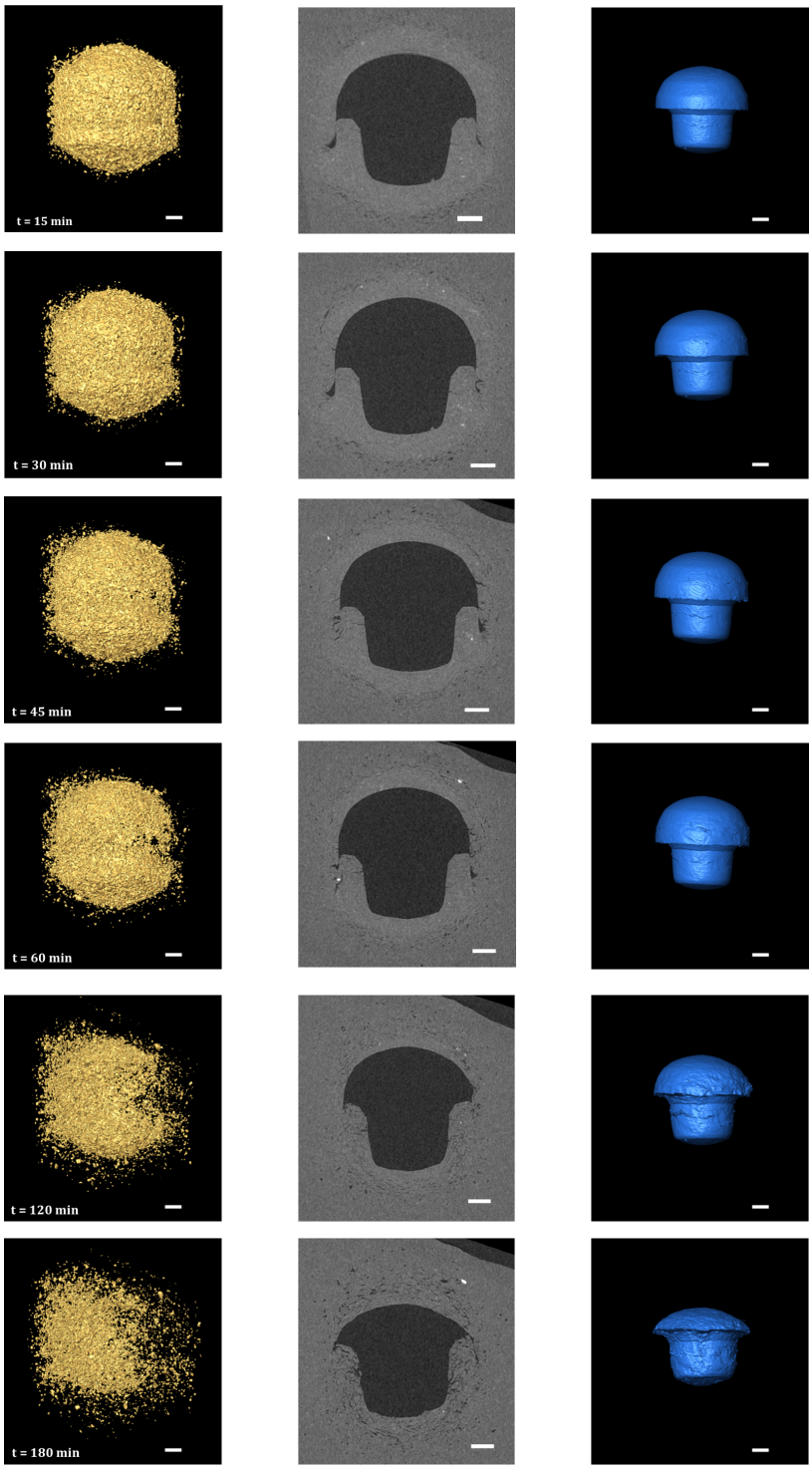

Figure 70. Left column: Images of X-ray tomography analysis of the 2 mg + 2 mg silodosin assembled system in void configuration at different times in pH 1.2; Central column: axial sections of the system and Right column: images of reconstruction of the empty space inside the assembled system.

The empty space inside the assembled system was reconstructed with computer (Figure 70, central column). The 3D images of the sample at different times are represented in the right column of Figure 70.

After immersion in the dissolution medium, the contour of the assembled system became less defined and same particles detached from the surface of the matrix system. As described by Losi et al [79], a disintegration of the surface took place before a consistent gel was formed. This phenomenon is due to the presence in the module formulation of high molecular weight HPMC. Both hydration and swelling processes of the polymer long chains are slow, thus the formation of a consistent gel layer is delayed enough to allow superficial disintegration to occur. As the contact time of the assembled system with the dissolution medium increases, a reduction in volume of the dense core is reduced while the gel layer increased in thickness.

The space occupied by air (darker area in the images of the central column) modified and decreased over time, due to the penetration of the solvent inside the assembled system. The internal area, measured with Image J, was 22.29 mm^2 and 17.25 mm^2 at 15 min and at 180 min, respectively.

The X-Ray computed tomography images of the assembled system made of three modules of silodosin 2 mg in mixed configuration (FFM: female/female/male modules) are reported in Figure 71. The initial disintegration of the surface of the assembled system caused the detachment of some particles.

The image sequence showed that the dense core reduced in volume and the individual particles or aggregates, detached from the dry core material, remained entrapped in the gel layer formed. The empty space inside the assembled system decreased until disappearing the one present between the two female modules (Figure 71, central column).

Similar behaviour is observed in the assembled systems of three modules of silodosin in FMF mixed configuration (Figure 72).

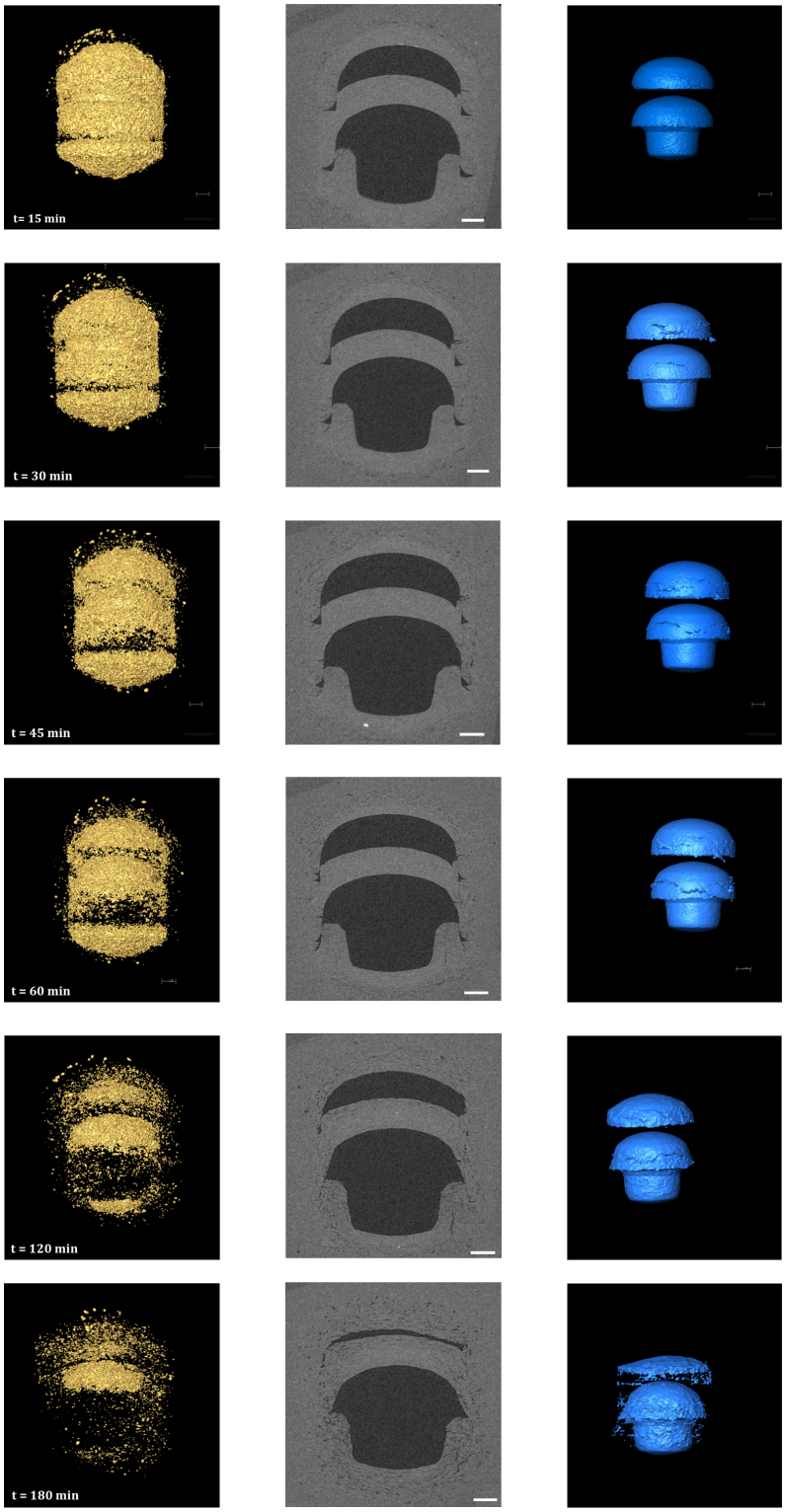

Figure 71. Left column: Images of X-ray tomography analysis illustrating the progressive swelling of the 2 mg + 2 mg + 2 mg silodosin assembled system in mixed configuration (FFM) at different times in pH 1.2; Central column: axial sections of the system and Right column: images of reconstruction of the empty space inside the assembled system.

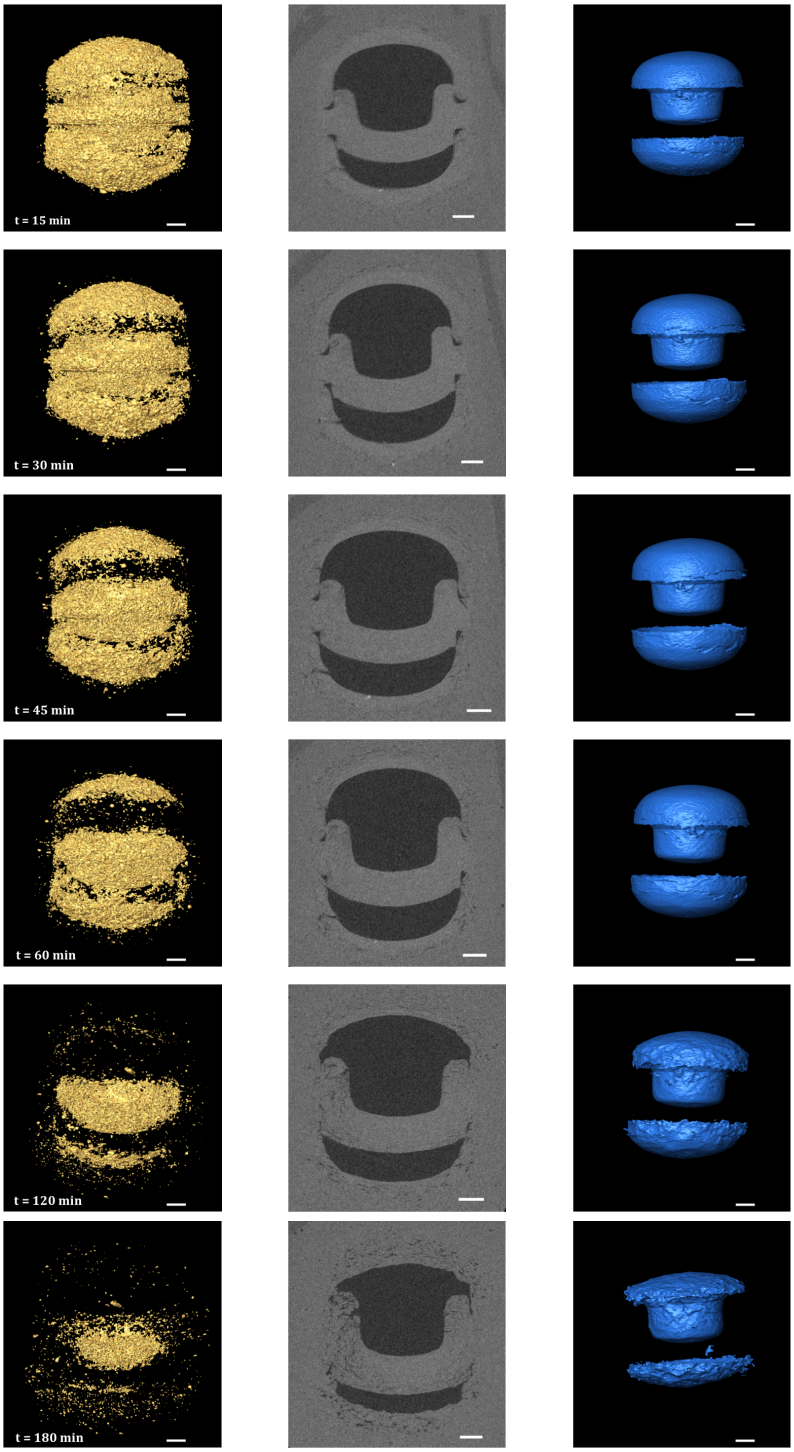

Figure 72. Left column: Images of X-ray tomography analysis of the 2 mg + 2 mg + 2 mg silodosin assembled system in mixed configuration (FMF) at different times in pH 1.2; Central column: axial sections of the system and Right column: images of reconstruction of the empty space inside the assembled system.

In Figure 73 the X-ray computed tomography images of the assembled system, made of silodosin 4 mg female module and sildenafil citrate 40 mg male module in void configuration, are reported. An evident change is observed at 45 min when some particles detached from the surface, especially in the female module of silodosin (upper), which dissolved before the sildenafil male module.

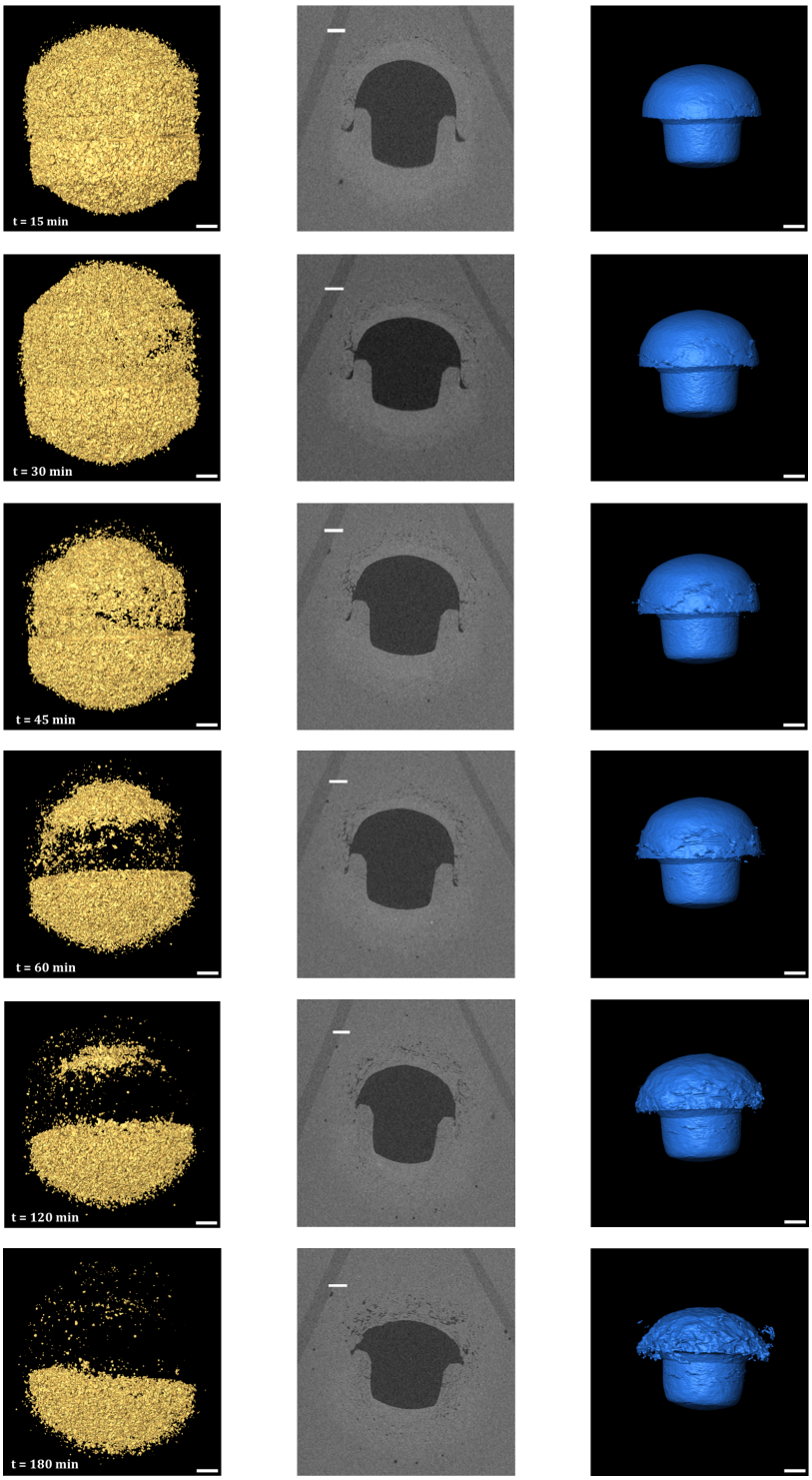

Figure 73. Left column: Images of X-Ray tomography analysis of the 4 mg silodosin female module/40 mg sildenafil citrate male module assembled in void configuration at different times in pH 1.2; Central column: axial sections of the system and Right column: images of reconstruction of the empty space inside the assembled system.

5. Conclusions

The present research work has been focused on the study of assembled system by Dome Matrix technology for the treatment of Benign Hyperplasia Prostatic. Dome matrix is a new platform for oral controlled drug release (rate and site control) characterised by two or more modules (male and female) assembled together in different configuration.

Flexible dosage forms of silodosin 4 mg, 6 mg or 8 mg were obtained. The *in vitro* dissolution tests evidenced that all the assembled systems floated and the release of silodosin from the assembled systems was at least 60% in the first 4 hours in acid medium (pH 1.2). The dissolution profiles at pH 3.5, instead, revealed a decrease of the release rate of silodosin mainly due to a reduction of drug solubility at this pH value.

The dissolution studies showed that the assembled systems containing 4 mg of silodosin exhibited a lower release rate when the drug was distributed on two modules instead one. This because of the ratio of drug and polymer in the two formulations was different. However, all the assembled systems of 4 mg released about 60% after 4 hours.

The assembled systems containing 6 mg of silodosin, obtained by different configurations (void and mixed configuration), did not evidence significant difference in the release of the drug.

The manufacturing of the individual release modules containing different dosage of the active principle and their assembled systems allows the

production of modified-release pharmaceutical forms containing a customizable dose of drug as a function of the therapeutic need.

A fixed dose combination product for the treatment of Benign Prostatic Hyperplasia was also investigated. The proposed combination is composed of silodosin and sildenafil citrate in a single dosage form gastro-retained. A module containing silodosin was assembled with a module containing sildenafil citrate in order to obtain a floating system. The objective of achieving a release of both drugs from the assembled systems at least 60% in the first 4 hours was reached at pH 1.2 from a specific combination of modules. In particular the system composed by sildenafil citrate female module and silodosin male module. The use of β-cyclodextrins for the manufacturing of sildenafil citrate modules gave promising result to increase the drug solubility in an acidic environment and thus facilitate the dissolution process of the module. The dissolution profiles at pH 3.5 of silodosin and sildenafil citrate by the individual modules and their assembled systems showed a decrease of the dissolution rate of both drugs. This is mainly due to the reduction of solubility for both silodosin and sildenfil citrate at this pH value.

The research project, carried out during the six months spent as a visiting student at the Department of Biomedical Engineering at University of Texas at Austin, was aimed to investigate the swelling behaviour of the individual modules and the assembled systems and to obtain a three-dimensional reconstruction of the assembled systems during the swelling process using the

X-ray computed tomography technique.

The study of the weight ratio during swelling demonstrated that the swelling of the female module was higher than the male module; this behaviour explains the higher dissolution rate from the female module with respect to the male module observed in the *in vitro* dissolution study.

The assembled systems showed lower and longer swelling ratio because of the less surface exposed to the dissolution medium as confirmed from the *in vitro* dissolution test. Moreover, the use of different dissolution media did not evidenced significant effects on the weight ratio during swelling of individual modules and their assembled system.

However, X-ray computed tomography technique applied to the study of dome matrix assembled, has allowed to better understand the internal modifications of the systems in the dissolution medium at different times.

6. References

1. Urinary System: Facts, Functions & Diseases by Kim Ann Zimmermann, Live Science Contributor, January 15, 2015 (imagine)
2. C. Dugdale, David. “Female urinary tract”. *MedLine Plus Medical Encyclopedia* (2011).
3. http://www.msdmanuals.com/home/SearchResults?query=urethra
4. Cunningham GR., Kadmon D. "Epidemiology and pathogenesis of benign prostatic hyperplasia." *UpToDate*; (2013).
5. Picture of “normal and enlarged Prostate”by Alan Hoofring (Illustrator), National Cancer Institute (2013).
6. Jepsen JV, Bruskewitz RC. Clinical manifestation and indications for treatment. In: Lepor H, editor. Prostatic Diseases. Philadelphia, PA: WB Saunders Co; pp. 123–142 (2000).
7. Berry SJ, Co ey DS, Walsh PC, Ewing LL. The development of human benign prostatic hyperplasia with age. *J Urol*;132 (3):474-9 (1984).
8. National Institute of Diabetes and Digestive and Kidney Diseases. Prostate enlargement: benign prostatic hyperplasia. NIH Publication No. 07-3012 (2006).
9. Roehrborn CG, McConnell JD. Etiology, pathophysiology, epidemiology and natural history of benign prostatic hyperplasia. In: Walsh PC, Retik AB, Vaughan ED Jr, Wein AJ, editors. Campbell’s Urology. 8th ed. Philadelphia, PA: WB Saunders Co; 2002. pp. 1297–1336.
10. Fenter TC, Naslund MJ, Shah MB, Eaddy MT, Black L. The cost of

treating the 10 most prevalent diseases in men 50 years of age or older. *Am J Manag Care*; 12 (4 Suppl):S90-S98 (2006).

11. Garraway WM, Collins GN, and Lee RJ: High prevalence of benign prostatic hypertrophy in the community. *Lancet* 338: 469 – 471, (1991).
12. Welch G, Weinger K, Barry MJ. Quality-of-life impact of lower urinary tract symptom severity: results from the Health Professionals Follow-up Study. *Urology*; 59(2): 245-50 (2002).
13. Wei JT, Calhoun E, Jacobsen SJ. Urologic diseases in america project: benign prostatic hyperplasia. *J Urol*; 179(5 Suppl):S75-80 (2005).
14. Kor MA, Bootman JL. The economics of benign prostatic hyperplasia treatment: a literature review. *Clin Ther*; 18(6): 1227-41 (1996).
15. http://www.urologyhealth.org/urologic-conditions/benign-prostatic-hyperplasia-(bph)/diagnosis
16. Silva J, Silva CM, Cruz F. "Current medical treatment of lower urinary tract symptoms/BPH: do we have a standard?" *Current opinion in urology* 24(1): 21-8 (2014).
17. Hutchison A; Farmer R; Verhamme K; Berges R; Navarrete R. "The Efficacy of Drugs for the Treatment of LUTS/BPH, A Study in 6 European Countries". *European Urology* 51(1): 207–16 (2007).
18. Djavan, Bob; Marberger, Michael. "A Meta-Analysis on the Efficacy and Tolerability of α_1-Adrenoceptor Antagonists in Patients with Lower Urinary Tract Symptoms Suggestive of Benign Prostatic Obstruction". *European Urology* 36(1): 1–13 (1999).
19. Oelke M, Bachmann A, Descazeaud M, Emberton S, Gravas MC, Michel

J, N'Dow J, Nordling JJ de la Rosette. Guidelines on the management of male lower urinary tract symptoms (LUTS), incl. benign prostatic obstruction (BPO). Available from: http://www.uroweb.org/gls/pdf/12_ Male_LUTS_after.corrections.pdf.

20. Novara G.; Ficarra V.; Zattoni F. "Medical treatment of LUTS/BPH" in Male LUTS/BPH Made Easy edited by C.R: Chapple and A. Tubaro, Springer (2014).
21. Santillo VM; Lowe FC."Treatment of benign prostatic hyperplasia in patients with cardiovascular disease". *Drugs and Aging* 10 (23): 795–805 (2006).
22. Gormley, Glenn J.; Stoner, Elizabeth; Bruskewitz, Reginald C.; Imperato-Mcginley, Julianne; Walsh, Patrick C.; McConnell, John D.; Andriole, Gerald L.; Geller, Jack; et al. "The Effect of Finasteride in Men with Benign Prostatic Hyperplasia". *New England Journal of Medicine* 327 (17): 1185–91 (1992).
23. Roehrborn, C; Boyle, P; Nickel, JC; Hoefner, K; Andriole, G; ARIA3001 ARIA3002 and ARIA3003 Study Investigators. "Efficacy and safety of a dual inhibitor of 5-alpha-reductase types 1 and 2 (dutasteride) in men with benign prostatic hyperplasia". *Urology* 60 (3): 434–41 (2002).
24. Roehrborn CG; Barkin J; Tubaro A; Emberton M; Wilson TH; Brotherton BJ; Castro R. "Influence of baseline variables on changes in International Prostate Symptom Score after combined therapy with dutasteride plus tamsulosin or either monotherapy in patients with benign prostatic hyperplasia and lower urinary tract symptoms: 4-year results of the

CombAT study.". *BJU international* 113 (4): 623–35 (2014).

25. Kaplan S; McConnell J; Roehrborn C; Meehan A; Lee M; Noble W; Kusek J; Nybergjr L. Medical Therapy of Prostatic Symptoms (MTOPS) Research Group. "Combination Therapy With Doxazosin and Finasteride for Benign Prostatic Hyperplasia in Patients With Lower Urinary Tract Symptoms and a Baseline Total Prostate Volume of 25 Ml or Greater". *The Journal of Urology* 175 (1): 217–20; discussion 220–1 (2006).
26. Gacci M; Ficarra V; Sebastianelli A; Corona G; Serni S; Shariat SF; Maggi M; Zattoni F; Carini M; Novara G. "Impact of medical treatments for male lower urinary tract symptoms due to benign prostatic hyperplasia on ejaculatory function: a systematic review and meta-analysis." *The journal of sexual medicine* 11 (6): 1554–66 (2014).
27. Kaplan S.A.; Roehrborn C.G.; Rovner E.S.; Carlsson M.; Bavendam T.; Guan Z. "Tolterodine and Tamsulosin for Treatment of Men With Lower Urinary Tract Symptoms and Overactive Bladder: A Randomized Controlled Trial". *JAMA: the Journal of the American Medical Association* 296 (19): 2319–28 (2006).
28. Abrams P; Andersson KE. “Muscarinic receptor antagonist for overactive bladder”. *BJU international* 100 (5): 987–1006 (2007).
29. Zenzmaier C, Sampson N, Pernkopf D, Plas E, Untergasser G, Berger P. Attenuated proliferation and trans-differentiation of prostatic stromal cells indicate suitability of phosphodiesterase type 5 inhibitors for prevention and treatment of benign prostatic hyperplasia. *Endocrinology*; 151(8):39 75-84 (2010).

30. Kaplan S.A., Gonzalez R.R. “Phosphodiesterase Type 5 Inhibitors for the Treatment of Male Lower Urinary Tract Symptoms” Rev Urol. 2007 Spring; 9(2): 73-77.
31. M. Yoshida, Y. Homma, K. Kawabe. “Silodosin, a novel selective alpha 1A- adrenoceptor selective antagonist for the treatment of benign prostatic hyperplasia”, *Expert Opin Investig Drugs* 16, p. 1955–65 (2007).
32. Kawabe K. “Current status of research on prostate-selective alpha 1-antagonists”, *Br J Urol.*; 81 (Suppl 1), p. 48–50 (1998).
33. Shibata K, Foglar R, Horie K, et al. “KMD-3213, a novel, potent, alpha 1a- adrenoceptor-selective antagonist: characterization using recombinant human alpha 1-adrenoceptors and native tissues”, *Mol Pharmacol* 48:250–258 (1995).
34. http://www.ema.europa.eu/docs/it_IT/document_library/EPAR_-_Product_Information/human/001092/WC500074180.pdf
35. Kawabe K, Yoshida M, Homma Y, for the Silodosin Clinical Study Group. “Silodosin, a new alpha1A-adrenoceptor-selective antagonist for treating benign prostatic hyperplasia: Results of a phase III randomized, placebo-controlled, double-blind study in Japanese men”, *BJU Int.*; 98:1019–1024 (2006).
36. European Medicines Agency. Silodyx (silodosin): EU summary of product characteristics. 2014. http://www.ema.europa.eu/, accessed 8/12/2014.
37. Zhou Y, Sun PH, Liu YW, Zhao X, Meng L, Cui YM “Safety and pharmacokinetic studies of silodosin, a new α1A-adrenoceptor selective antagonist, in healthy Chinese male subjects. *Biol Pharm Bull.;*

34(8):1240-5 (2011).

38. http://www.fda.gov

39. Webb, D.J.; Freestone, S.; Allen, M.J.; Muirhead, G.J. "Sildenafil citrate and blood-pressure-lowering drugs: results of drug interaction studies with an organic nitrate and a calcium antagonist". *Am. J. Cardiol.* 83 (5A): 21C–28C (1999).

40. McVary K.T., Monnig W., Camps J.L., Young J.M., Tseng L.J., van den Ende G. “Sildenafil citrate Improves Erectile Function and Urinary Symptoms in Men with Erectile Dysfunction and Lower Urinary Tract Symptoms Associated with Benign Prostatic Hyperplasia: A Randomized, Double-Blind Trial.” *J.Urol.* 177, 1071-77 (2007).

41. Lepor H. Advances in the medical treatment of benign prostatic hyperplasia. *Reviews in Urology* 11, 181-184 (2009).

42. Filippi S., Morelli A., Sander P., Fibbi B., Mancina R., Marini M., Gacci M., Vignozzi L., Vannelli GB., Carini M., Forti G., Maggi M., “Characterization and functional role of androgen-dependent PDE5 activity in the baldder”. *Endocrinology* 148 (3), 1019-1029 (2007).

43. Nichols D.J., Muihead G.J., Harness J.A. Pharmacokinetics of sildenafil after single oral doses in healthy male subjects: absolute bioavailability, food effects and dose proportionally. *Br. J. Clin Pharmacol* 53, 5S-12S (2002).

44. Osman M.A., El Maghraby G.M., Hadaya M.A. Intestinal absorption and presystemic disposition of sildenafil citrate in the rabbit: evidence for site-

dependent absorptive clearance. *Biopharm. Drug Disp.* 27, 93-102 (2006).

45. MacDiarmid S., Hill L.A., Volinn W., Hoel G. Lack of Pharmacodynamic interaction of silodosin, a highly selective α1a-adrenoceptor antagonist, with the phosphodiesterase-5 inhibitors sildenafil and tadalafil in healthy men. *Urol.* 75, 520-525 (2010).
46. Desphande, A.A.; Rhodes, C.T.; Shah, N.S.; Malick, A.W. Controlled-release drug delivery systems for prolonged gastric residence: An overview. *Drug Dev. Ind. Pharm.* 22, p.531-539 (1996).
47. J. R. Robinson, V.H K. Li, V. H. L. Lee, *Influence of drug properties and routes of drug administration on the design of sustained and controlled release systems,* Controlled Drug Delivery Fundamentals and Applications, second ed., Marcel Dekker Inc., New York, (1987).
48. P. Colombo, P. Santi, R. Bettini, C. Brazel, N.A. Peppas, *Drug release from swelling-controlled systems*, in Wise D. (ed.), Handbook of Pharmaceutcal Controlled Release Thecnology, Dekker, New York, , 9, p. 183-206 (2000).
49. R.W. Korsmeyer, N.A. Peppas, "Macromolecular and modeling aspect of swelling-controlled system", Rosemann T.J., Mansdorf S.Z., *Controlled Release Delivery Systems*, Dekker ed., New York and Basel, (1983).
50. P. Colombo, "Swelling-controlled release in hydrogel matrices for oral route*" Adv Drug Del*, Rewiew, 11, p. 37-57 (1993).

51. P. Borgquist, A. Körner, L. Piculell, A. Larsson, A. A Axelsson, “A model for the drug release from a polymer matrix tablet—effects of swelling and dissolution”*, J Control Release*, 113 (3), p. 216-25 (2006).
52. A. Frank, S. K. Rath, S. S. Venkatraman, “Controlled release from bioerodible polymers: effect of drug type and polymer composition”, *J Control Release*, 102 (2), p. 333-44 (2005).
53. P. M. de la Torre, S. Torrado, S. Torrado, *Interpolymer complexes of poly (acrili acid) and chitosan: influence of the ionic hydrogel-forming medium,* Biomaterials, 24 (8), p. 1459-68 (2003).
54. P. Colombo, R. Bettini, P.L. Catellani, P. Santi, N. A. Peppas, *Drug volume fraction profile in the gel phase and drug release kinetics in hydroxypropylmethyl cellulose matrices containing a soluble drug*, Eur J Pharm Sci, 9 (1), p. 33-40 (1999).
55. Tiwari, S., J. DiNunzio, and A. Rajabi-Siahboomi, *Drug-Polymer Matrices for Extended Release*, in *Controlled Release in Oral Drug Delivery SE - 7*, C.G. Wilson and P.J. Crowley, Editors. 2011, Springer US DA - p. 131-159 (2011).
56. P. Colombo, R. Bettini, P.L. Catellani, P. Santi, N. A. Peppas, *Drug volume fraction profile in the gel phase and drug release kinetics in hydroxypropylmethyl cellulose matrices containing a soluble drug*, Eur J Pharm Sci, 9 (1), Oct 1999, 33-40.
57. T. Phaechamud, “Variables influencing drug release from layered matrix system comprising hydroxypropyl methylcellulose”*, AAPS PharmSciTech*, 9 (2), p. 668-74 (2008).

58. P. Colombo, P. Santi, J. Siepmann, G. Colombo, F. Sonvico, A. Rossi, O.L. Strusi, *Swellable and Rigid Matrices: Controlled Release Matrices with Cellulose Ethers*, Pharmaceutical Dosage Forms: Tablets, Third Edition, Edited by Larry L. Augsburger, Stephen W. Hoag, 2008, vol. 2, cap. 14.
59. A.T. Pham, P.I. Lee, *Probing the Mechanism of Drug Release from Hydroxypropylmethyl Cellulose Matrices,* Pharmaceutical Research, 11 (10), 1994, 1379-1384.
60. P. Colombo, R. Bettini, P. Santi, N. A. Peppas, *Swellable matrices for controlled drug delivery: gel-layer behaviour, mechanisms and optimal performance*, Pharm Sci Technol Today, 3 (6), Jun 2000, 198-204.
61. P.I. Lee, N.A. Peppas, *Prediction of polymer dissolution in swelling controlled-release systems,* J Control Release, 1987, 207-215.
62. P. Colombo, R. Bettini, N.A. Peppas, *Observation on swelling process and diffusion fron position during swelling in hydroxypropylmethyl cellulose (HPMC) matrices containing a soluble drug*, J Control Release, 61, 1999, 83- 91.
63. P. Colombo, R. Bettini, G. Massimo, P.L.Catellani., P. Santi, N.A. Peppas, *Drug diffusion front movements is important in drug release control from swellable matrix tablets*, J Pharm Sci, 84, 991-997 (1995).
64. Colombo P., Bettini R., Peppas N.A. “Observation of swelling process and diffusion front position during swelling in hydroxypropyl methyl cellulose (HPMC) matrices containing a soluble drug” *Journal of Controlled Release* 61, p. 83–91 (1999).

65. Colombo, P., *Swelling-controlled release in hydrogel matrices for oral route.* Advanced Drug Delivery Reviews, Modern Hydrogel Delivery Systems, 1993. **11**(1-2): p. 37-57.
66. R. Bettini, P. L. Catellani, P. Santi, G. Massimo, N. A. Peppas, P. Colombo, “Translocation of drug particles in HPMC matrix gel layer: effect of drug solubility and influence on release rate”, J Control Release, 70 (3), Feb 2001, 383-91.
67. Peppas, N.A. and Colombo, P., “Analysis of drug release behavior from swellable polymer carriers using the dimensionality index. Journal of controlled Release, 45 (1), p. 35-40, (1997).
68. Ritger, P.L. and N.A. Peppas, A simple equation fro description of solute release I. Fickian and non-fickian release from non-swellable devices in the form of slabs, spheres, cylindres or discs. Journal of Controlled Release, 5 (1): p.23-36, (1987).
69. Ritger, P.L. and N.A. Peppas, A simple equation fro description of solute release II. Fickian and anomalous release from swellable devices. Journal of Controlled Release, 5 (1): p. 37-42, (1987).
70. Peppas, N.A., *Analysis of Fickian and non-Fickian drug release from polymers.* Pharmaceutica acta Helvetiae, 1985. 60(4): p. 110-111.
71. Peppas, N.A. and R.W. Korsmeyer, *Dinamically swelling hydrogels in controlled release applications*, in *Hydrogels in Medicine and Pharmacy*, N.A. Peppas, Editor. 1986, CCR Press. p. 109-136.

72. Peppas, N.A. and J. Sahlin, “A simple equation of for the description of solute release. III. Coupling of diffusion and relaxation”. International Journal of Pharmaceutics 57: p. 169-172 (1989).
73. Benetti C., Colombo P., T.W. Wong “Cellulose-, Ethylene Oxide- and Acrylic-Based Polymers in Assembled Module Technology (Dome Matrix) in “Handbook of polymers for Pharmaceutical Technologies, Vol 3 Biodegradable Polymers” edited by V. Kumari Thakur; M. Kumar Thakur; Wiley (2015).
74. Losi E, Bettini R, Santi P, Sonvico F, Colombo G, Lofthus K, Colombo P, Peppas NA. “Assemblage of novel release modules for the development of adaptable drug delivery systems*”. Journal of Controlled Release* 111, Issues 1-2, p. 212-218 (2006).
75. O.L. Strusi, F. Sonvico, R. Bettini, P. Santi, G.Colombo, P.Barata, A. Oliveira, D. Santos, P. Colombo. “Module assemblage tecnology for floating systems: In vitro flotation and in vivo gastro-retention”. *J. Contr. Rel*., 129, p. 88- 92 (2008).
76. C. Hascicek, A. Rossi, P. Colombo, G. Massimo, O.L. Strusi, G. Colombo. “Assemblage of drug release modules: Effect of module shape and position in the assembled systems on floating behavior and release rate”. *European Journal of Pharmaceutics and Biopharmaceutics* Volume 77, Issue 1, p. 116-121 (2011).
77. SS Davis, JG Hardy, JW Fara, Transit of pharmaceutical dosage forms through the small intestine*, Gut*, 27, 886-892 (1986).

78. G. Darwiche, E. M. Östman, H. GM Liljieberg, N. Kallinen, I. ME Björck, L.O. Almér, Measurements of the gastric emptying rate by use of ultrasonography: studies in humans using bread with added sodium propionate*, Am J Clin Nutr,* 74, p. 254-8 (2001).

79. E. Losi, N.A. Peppas, R.A. Ketcham, G. Colombo, R. Bettini, F. Sonvico, P. Colombo “Investigation of swelling behavior of Dome Matrix drug delivery modules by high resolution X-ray computed tomography” J. Drug Del. Sci. Tech, 23 (1) 165-170 (2013).